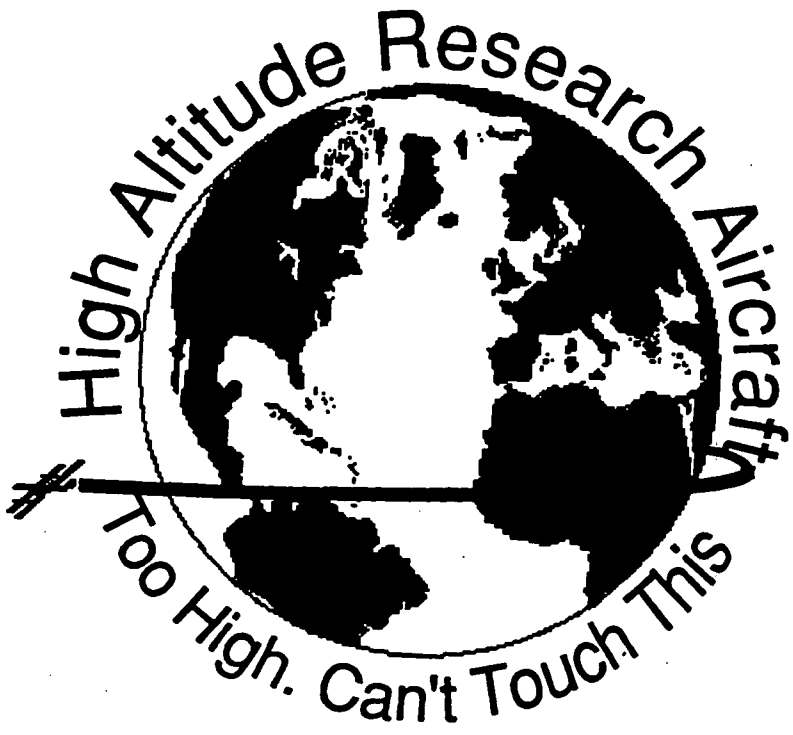

California State Polytechnic University, Pomona
Department of Aerospace Engineering

The HAMMER:

High **A**ltitude **M**ultiple **M**ission **E**nvironmental **R**esearcher

Group Leaders:
Darren Hayashi
Cara Zylla

Team Members:
Ernesto Amaro — Configurations
Phil Colin — Structures/Materials
Thomas Klause — Propulsion/Performance
Bernardo Lopez — Weights/Subsystems
Danna Williamson — Aerodynamics

May 1991

The Known is finite, the unknown infinite; intellectually we stand on an islet in the midst of an illimitable ocean of inexplicability. Our business in every generation is to reclaim a little more land.

-T.H. Huxley,1887

The final typesetting and editing of the manuscript is attributed to:
Darren K. Hayashi and Thomas D. Klause

This report was set in Helvetica 12 point
Using Aldus Pagemaker 4.0 for the Apple Macintosh

Special Thanks to J. Randolph and M. Coleman for computer access

California State Polytechnic University, Pomona
3801 West Temple Avenue
Pomona Ca 91768

May 28,1991

I. ABSTRACT

At the equator, the ozone layer ranges from 65,000 to 130,000+ feet which is beyond the capabilities of the ER-2, NASA's current high altitude reconnaissance aircraft. The Universities Space Research Association, in cooperation with NASA, is sponsoring an undergraduate program which is geared to designing an aircraft that can study the ozone layer at the equator. This aircraft must beable to satisfy four mission profiles. Mission one is a polar mission which ranges from Chile to the South Pole and back to Chile, a total range of 6000 n. mi at 100,000 feet with a 2500 lb. payload. The second mission is also a polar mission with a decreased altitude of 70,000 feet and an increased payload of 4000lb. For the third mission, the aircraft will take-off at NASA Ames, cruise at 100,000 feet carrying a 2500 lb. payload, and landin Puerto Montt, Chile. The final mission requires the aircraft to take-off at NASA Ames, cruise at 100,000 feet with a 1000 lb. payload, make an excursion to 120,000 feet, and land at Howard AFB,Panama. All three missions require that a subsonic Mach number bemaintained due to constraints imposed by the air sampling equipment. The aircraft need not be manned for all four missions. Three aircraft configurations have been determined to be the most suitable for meeting the above requirements. The performance of each configuration is analyzed to investigate the feasibility of the project requirements. In the event that a requirement can not be obtained within the given constraints, recommendations for proposal modifications are given.

Contents

1.0 Introduction
1.1 Study Activities 1
1.2 Mission Profile Summary 2
1.3 Aircraft System Requirements 3

2.0 Science
2.1 The Earth's Atmosphere 6
2.1.1 Division of the Atmosphere 7
Table 2.1:The Standard Atmosphere at Significant Mission Altitudes 7
2.1.2 The Ozone Depletion Problem 8
Figure 2.1: Cycle of Ozone Depletion 9
2.2 High Altitude Research Instrumentation 11
2.3 Payload Arrangement 12
2.4 Telecommunication, Navigation and Data Handling 13
Table 2.2: XR-1 Payload Distribution and Weights 14

3.0 Mission Design
3.1 Mission Profiles Summary 16
3.1.1 Baseline Mission Profile 1 17
Figure 3.1: Polar Mission 18
3.1.2 Reduced Altitude Mission Profile 2 18
Figure 3.2: Polar Mission 2 19
3.1.3 Midlatitude Mission 3 20
Figure 3.3: Midlatitude Mission 3 20
3.1.4 Midlatitude Zoom Mission 4 21
Figure 3.4: Zoom Mission 4 22
3.1.5 Manned Vs. Unmanned Flight 22
3.2 Aircraft Performance Analysis 23
3.2.1 Takeoff Phase 23
3.2.2 Climb Phase 24
Figure 3.5 :XR-1 Power Required Profile for Baseline Mission 25
Figure 3.6: XR-1 Flight Envelope 26
3.2.3 Cruise Phase 26
3.2.4 Landing Phase 27
3.3 Mission RFP Requirements 27
Table 3.1: Mission Profile Summary 28

4.0 Aircraft Design

4.1 Configuration 29
4.1.1 Conventional 29
Figure 4.1: Conventional Aircraft Configuration 31
4.1.3 Joined Wing 31
Figure 4.3: Joined Wing Configuration 31
4.1.4 Canard 33
Figure 4.4: Canard Aircraft Configuration 33
4.1.5 Biplane 34
Figure 4.5: Biplane Aircraft Configuration 34
4.1.6 Twin Fuselage 35
4.1.7 Twin Boom 35
Figure 4.6: Twin Boom/Twin Fuselage Aircraft Configurations 36
4.1.8 Tandem Wing 36
4.2 Configuration Finalists 38
Figure 4.8: Tandem Wing Configuration 38
4.3 Final Configuration 39
Table 4.1: Aircraft Geometric Parameters: 40
4.4 Mission System Requirements 41
4.4.1 Telemetry Systems 42
4.4.2 Power System 42
4.4.3 Stability Augmentation Systems 42
4.4.4 Fuel System 42
4.4.5 Heat Dissipation/Anti–icing Systems 43
4.4.6 Data Acquisition System 43
4.4.7 Land Support Systems 44
4.5 Weight Estimation 44
Table 4.2: Preliminary Weight Estimation 44
Table 4.3: Component Weight Breakdown 45

5.0 Aircraft System Functional Descriptions

5.1 Aerodynamics 47
5.1.1 Airfoil Analysis 47
5.0 System Functional Descriptions 47
5.1.2 Reynolds Number 48
5.1.3 Airfoil Selection 50
5.1.4 Aircraft Aerodynamics 52
Figure 5.1: Wing Reference Area vs. Mach Number 53
Figure 5.3: Wing Reference Area vs. Total Drag 53
Figure 5.4: Lift Coefficient & Drag Vs. Mach Number 55
Figure 5.5: Wing Reference Area vs.Total Drag 56
5.2 Structures and Materials 58
Figure 5.6: XR-1 Structural Planform 61

Figure 5.7: XR-1 Wing Structure 63
5.8: XR-1 Vertical Tail Structure 64
5.2.1 Aircraft Operational Envelope 65
Figure 5.9: XR-1 V-n Diagram. 66
5.3 Aircraft Propulsion System 66
5.3.1 Propulsion Options 66
5.3.2 Turbine Engines 67
5.3.3 Internal Combustion Engine 68
Figure 5.10: Turbocharging Schematic 69
5.3.4 Solar Power 69
5.4 XR-1 Engine Selection 70
Figure 5.11: TCM TSIOL 550 Schematic 71
5.4.1 Engine Cooling 73
5.5 Power Requirement Determination 74
5.6 Propeller Design 75
Figure 5.12: Advanced Propfan Propeller 76
5.7 Aircraft Stability and Control 77
5.7.1 Aircraft Stability Derivatives 78
Table 5.3.1: Summary of Flight Phases 78
5.7.2 Longitudinal Static Stability 79
Table 5.4.2: Summary of Longitundial Stability Derivatives 79
5.7.3 Longitudinal Dynamic Stability 80
Table 5.5: Lateral Stability Derivatives 80
5.7.4 Lateral Dynamic Stability 81
Table 5.6: Uncompensated Longitudinal/Lateral Modes 81
5.7.5 Stability Augementation Systems 82
5.7.6 Autopilots 82
Figure 5.13: Pitch Displacemnt Auto Pilot 83
Figure 5.14 Mach Hold Autopilot 84
Figure 5.15: Intergrated Fliight Control System 86
5.8 Landing Gear 86
Figure 5.16: XR-1 Landing Gear Configuration 88
5.9 Ground Handling 89
5.10 Crashworthiness 90
5.11 Maintainability 91

6.0 Program Planning

6.1 Budget Considerations 97
Table 6.1: Cost Estimations 98
Table 6.2: Cost Estimations 98
6.2 Design Program Plans 99
Figure 6.1: XR-1 Program Milestones 100
6.3 Manufacturing 102

7.0 Summary

7.1 Analysis Overview 106
Table 7.1: RFP Comparsion Chart 107
7.2 Aircraft Design Summary 108
7.3 Concluding Remarks 109

1.0 Introduction

1.1 Study Activities

The Earth is surrounded by a gaseous envelope known as the atmosphere. The atmosphere contains the air its inhabitants breathe and helps keep the surface climate habitable. In the mid layer of the atmosphere there exists a layer of ozone which acts as a blanket wrapped around the Earth protecting both animal and plant life on the surface from fatal ultraviolet rays. As long as this ozone layer surrounds the Earth, the environment will remain stable, but any change in this steady state could be catastrophic. Unfortunately, it has recently been discovered that the ozone layer is diminishing, and that losses, amounting to as much as 50% under certain conditions, have been experienced. Many questions remain unanswered about the chemical composition of the atmosphere at these altitudes and will remain unanswered until a research platform is created that can gather the necessary data. It is for this reason that the National Aeronautics and Space Administration (NASA) is funding the research and possible development of a vehicle that can perform this task. California State Polytechnic University, Pomona's USRA design team hereby proposes an aircraft capable of cruising at an altitude of 100,000 feet for a range of

6000 nautical miles, sampling the atmosphere at altitudes higher than present technology allows. The XR-1 High Altitude Multiple Mission Environmental Researcher (HAMMER), discussed in detail on the following pages, is the HAMMER team's solution to this problem.

1.2 Mission Profile Summary

The mission design objectives were to develop an aircraft capable of flying at altitudes as high as 100,000 feet, with possible zoom up to 120,000 feet desired. The aircraft is to be equipped with scientific payload consisting of the instrumentation necessary to sample the chemistry of the ozone layer at this altitude. Four basic mission profiles are to be considered as shown in Section 3.

- Polar Mission 1: (Chile to South Pole to Chile: 6000 n mi @ 100,000 ft)
- Polar Mission 2: (Chile to South Pole to Chile: 6000 n mi @ 70,000 ft)
- Midlatitude Mission 3: (NASA Ames to Chile: 6000 n mi @ 100,000 ft)
- Zoom Mission 4: (NASA Ames to Panama: 3250 n mi w/ zoom to 120,000ft)

It was determined that three of the four mission profiles specified above were attainable without modification. A maximum cruise altitude of 100,000 ft exists with a zoom up potential to 111,000 ft. Each specific mission profile and the aircraft performance will be considered in turn in Section 3.0.

1.3 Aircraft System Requirements

The requirements for the aircraft as presented in the Request for Proposal (RFP) are as follows:

- The aircraft in question must perform four specified missions, to be discussed in detail in Section Three.
- The aircraft must be capable of flying at an altitude of 100,000 feet, subsonically, for a range of 6000 nautical miles carrying a payload of 2500 pounds.
- If the aircraft is manned, it must have redundant life support systems and be pilot friendly. If the aircraft is to be unmanned, it must be proved to the satisfaction of both the scientists and the designers that this is the better alternative.
- The aircraft must be able to operate from at least the runways specified in the mission profile.
- The aircraft must be able to withstand atmospheric crosswinds of up to 15 knots, with moderate to severe turbulence.
- Spoilers or alternative lift dump devices are to be provided for the low wing loading landing of the aircraft.
- A minimum of two engines is required for safety and flexibility of the aircraft.
- The aircraft must be able to fit into a hangar of size 110 ft x70 ft.
- The aircraft must be able to enter production before the year 2000.

Fulfilling all of these requirements is not as simple as it appears. The first step in the design process is to identify the major design drivers, that is, it must be decided which areas are the most critical to the design. The major areas of concern for this project (the design drivers) include the propulsion system, structural and weight considerations for the aircraft, aerodynamics/airfoil selection, and the stability and control system for the aircraft.

First, the propulsion system provides a special design challenge in itself due

to the fact that the density of air at an altitude of 100,000 feet is much less than the air density at sea level. This restricts the compressor pressure ratios from this dramatic decrease in air density if a conventional type of aircraft engine is to be used. It also may inhibit combustion due to the lack of oxygen at altitude. Furthermore, engine cooling becomes a major consideration at the higher altitudes.

Second, the weight of the aircraft cannot be too great. The more the aircraft weighs, the more difficult it will be and the more power it will take to get the aircraft up to 100,000 feet, without experiencing transonic flight regime. This puts a burden on the structure of the aircraft, if you will, by restricting the percentage of the gross take-off weight that may be used for structures. Yet the aircraft must be large enough and strong enough to carry payloads of up to 4000 pounds and possibly tolerate wing spans rivaling that of a Boeing 747 for a fraction of the weight.

Next, the aerodynamics of the aircraft becomes a major issue when it is discovered that an exceedingly large lift coefficient is required as is a low Reynolds number airfoil. This must all be achieved while minimizing the drag as much as possible. This is difficult to do given a large surface area, and the large wing area that is required to produce the lift that is necessary to reach such high altitudes.

Finally, the stability of the aircraft and the control systems that are to be used for the aircraft prove to be another design driver. It is probable that the aircraft will not be stable without some method to help control the aircraft using either control surfaces or stability augmentation systems. However, caution must be taken during the design process to not make the aircraft too unstable, for it is possible for the aircraft to be uncontrollable, in which case no amount of stabilization (artificial or otherwise) will make the plane stable. If this were to be the case, the entire design process would be wasted and the aircraft would have to be wholly redesigned.

Faced with the above challenges, the design of a subsonic, high altitude

aircraft was begun. This report is the culmination of the research and analysis for the California State Polytechnic University, Pomona HAMMER Design Team. The proposal describes both the design process and future studies for the experimental research aircraft, the XR-1 High Altitude Multiple Mission Environmental Researcher (HAMMER).

2.0 Science

The intent of this section is to briefly describe the Earth's atmosphere, particularly in the regime of interest for this project, and the ozone depletion problem that merits this study. In addition, the XR-1's scientific instrumentation and possible payload configurations of these instruments will be examined. This will serve to give an overview of why the problem exists and why NASA is considering the development of a high altitude subsonic research aircraft.

2.1 The Earth's Atmosphere

In any design, it is important to know under what conditions the finished project is expected to perform , whether it be the road conditions for a new automobile, or the atmospheric conditions for an airplane as is the case here. Since it is desired to achieve altitudes in excess of 100,000 feet, it is desirable to know what to expect throughout all altitudes. The majority of the mission entails flying subsonically at altitudes above 70,000 ft which is heretofore unheard of, so these atmospheric conditions are of primary importance in the design and are discussed below.

2.1.1 Division of the Atmosphere

The Standard Atmosphere for several of the major altitudes which the XR-1 will reach are summarized in Table 2.1. It is noted that the temperature decreases with altitude until the stratosphere is reached, at which point an isothermal region is encountered. This constant temperature exists through the beginning of the upper stratosphere (80,000 ft) at which point the temperature increases with additional altitude. This temperature flux is important due to the dependance of Mach number on temperature.

Most conventional aircraft operate solely in the troposphere. This is a region in which the XR-1 will encounter only briefly on its way towards cruise wihtin the upper stratosphere (100,000 ft). The aircraft will be designed primarily around cruise conditions, that is at a Standard Atmosphere of 100,000 ft.

Table 2.1:The Standard Atmosphere at Significant Mission Altitudes

Altitude (ft)	Temp. (°R)	Pressure (psf)	Density (slug/ft3)	Viscosity (ft2/sec)
0	518.7	2.1162e3	2.3769e-3	1.5723e-4
10000	483.0	1.4556e3	1.7556e-3	2.0132e-4
30000	411.9	6.2966e2	8.9068e-4	3.4882e-4
50000	390.0	2.4361e2	3.6391e-4	8.1587e-4
70000	390.0	9.3672e1	1.3993e-4	2.1434e-3
100000	418.8	2.3085e1	3.2114e-5	9.3017e-3
120000	451.4	9.8372e0	1.2697e-5	2.4197e-2

2.1.2 The Ozone Depletion Problem

The ozone layer acts like a protective blanket wrapped around the Earth, protecting life on its surface and warming the upper atmosphere. Ozone, being an opaque particle, protects surface life by absorbing ultraviolet (UV) rays from the sun, a unique property of the compound. By absorbing the sun's rays, ozone creates the stratosphere, where the temperature rises with altitude, regulating worldwide circulation patterns and keeping weather confined below in the troposphere. Ozone, which comes from the Greek word "ozien," meaning to smell, is a natural product of sunlight acting on diatomic oxygen in the upper atmosphere. It is transported vertically from the upper stratosphere where it is produced, to the lower stratosphere, and horizontally by the meteorological conditions and geography. The poles have the highest concentration of ozone due to the lesser amount of direct sunlight (UV) they receive in comparison to the equatorial regions. In the lower stratosphere and at the poles, less ozone is produced because the ultraviolet rays must travel through more air due to the tilt of the Earth about its axis.

Ozone (O_3), is an unstable molecule, always willing to give up one of its oxygen atoms to other gases to reform diatomic oxygen (O_2), and an oxygen compound with another atom or group of atoms. Unfortunately, this instability is ozone's nemesis as will be seen shortly. Ozone is created when ultraviolet radiation or discharges of electricity (lightning) split O_2 molecules into two single oxygen atoms which link with unsplit O_2 molecules to form the unstable ozone. Only certain chemicals break down the ozone; unfortunately they tend to be quite popular and marketable. The prime destructors are Chloroflourocarbons (CFCs), Bromine Oxides, and Nitrogen Oxides. To better understand the problem, a simple model of the destruction process is now illustrated.

The energy of the sun in the stratosphere which broke up the diatomic oxygen is also strong enough to dissociate the chlorine from the CFC. This chlorine is then free to collide with the unstable ozone molecule and form diatomic oxygen and another unstable compound, chlorine monoxide (ClO). The oxygen atom in the ClO can then react with the free oxygen atoms in the stratosphere, leaving the chlorine atom free to begin the cycle again. Therefore, a breakup of one CFC by UV can set off a catalytic chain in which one chlorine atom could potentially destroy 100,000 ozone molecules.

Thus every cycle will destroy two ozone molecules. Figure 2.1 pictures this cycle in six stages.

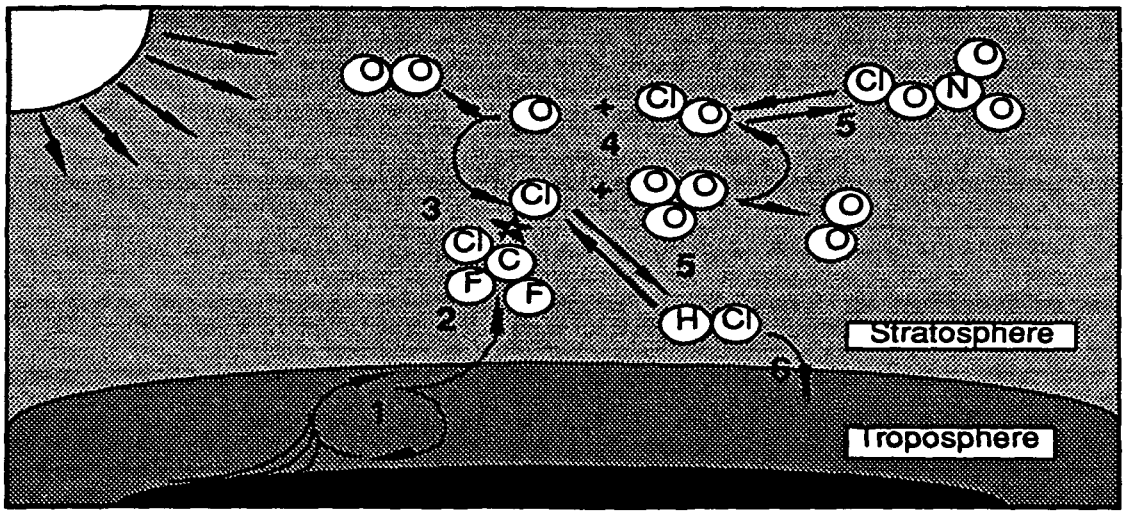

Figure 2.1: Cycle of Ozone Depletion

1. Release of CFCs and circulation through the troposphere
2. Slow mixing into the stratosphere
3. UV attack on CFC and liberation of Cl atom
4. Rapid catalytic cycle that destroys ozone

5. Temporary end of ozone destruction due to Cl conversion into a stable molecule (eventually the ClO will once again be released.)
6. Mixing of chlorine with hydrogen, HCl, back into the troposphere (rain).

The depleting tendencies of the above listed particles can and will have a catastrophic effect on all civilization and life if precautions are not taken immediately. As the ozone diminishes, more ultraviolet (UV) light will pass through the tropopause on to the planet's surface. This excess in UV rays will effect plant and animal life alike. An increase in UV light means a large increase of reported skin cancer cases and thus an increase in cancer related deaths. It will vastly reduce crop yields and will severely disrupt the aquatic food chain by killing plankton, the smallest element of this chain. Scientists predict that a mere 1% reduction in ozone will result in a 2% increase in UV radiation and cause a 5% to 8% increase in the number of skin cancer cases worldwide.

It is now quite apparent that a problem exists. In order to understand the process that occurs, sampling of the atmosphere up to 100,000 feet and beyond is needed to model the time scale and movement of CFCs, answering some puzzling questions.

- What causes ozone loss above the dehydration region in Antarctica?
- To what extent are dehydration, denitrification and ozone loss transmitted to populous midlatitudes?
- What are the abundances and the gradients of the following within the vortex? O_3, ClO, Cl_2O_2, BrO, NO, NO_2, OH, HO_2?
- What maintains the geographical distribution of polar strato spheric clouds, and how do they transform the chemical balance as a function of temperature and pressure?
- How do polar stratospheric clouds and their underlying decks of high, cold cirrus affect the vertical motion field?

These are but a few questions that remain unanswered. With the implementation of a high altitude research platform, hopefully all of these questions will be answered in time that we may salvage the atmosphere, and thus the life on the planet which it surrounds.

In order to answer these questions, a detailed scientific research platform for the aircraft needs to be assembled. Section 2.2 will focus on the payload required for the XR-1 mission.

2.2 High Altitude Research Instrumentation

In order to measure the concentration of different elements in the atmosphere it is necessary to incorporate an assembly of test equipment as the plane's payload. For the proposed aircraft, the payload will consist of both sensors and in situ samplers. Due to the effectiveness of the results obtained by the ER-2, NASA's present high altitude research platform, sensing equipment on the newly proposed aircraft should remain similar. The only extra foreseen limitation is the new aircraft's increase in altitude up to levels as high as 110,000 feet above the Earth's surface. The present ER-2 technology is designed for operation at altitudes at a maximum of only 70,000 feet. The primary concern will be to modify the existing equipment to withstand the extreme low pressures of the upper stratosphere.

Critical issues in the study of polar stratospheric chemistry, physics, chemical elements transported by global circulation, and the Earth's radiation balance can be addressed by use of remote sensors and in situ (fixed position) instrumentation . Remote sensing uses either active or passive techniques in its method of taking atmospheric data. Active sensing uses a light source, usually a laser, as the sensing part of the equipment. The laser is then able to make measurements which are

independent of scattered light. This technique provides high spatial resolution profiles at a range of up to 20 km above or below the aircraft. This technique is used primarily for the measurement of the concentrations of ozone, water vapor, and aerosols or clouds of other chemicals. In contrast, passive sensing is conducted by either viewing the sun directly, or detecting the scattered sunlight. A common practice is to use infrared emissions from gases in the atmosphere, allowing night or day use. This technique is used in measuring trace stratospheric gases and radiation. With the sensors in operation, the data is collected by an on board data processor and is sent to ground control centers by two way telemetry allowing real time mission decisions to be made. This will provide the advantage of being able to change the mission directives while in flight in order to follow calculated in situ sampling strategies. The complement of remote sensing methods in conjunction with a comprehensive set of in situ measurements is necessary. A more detailed listing of the science instruments carried as well as its orientation on the aircraft is provided Section 2.3.

2.3 Payload Arrangement

The required payload for the baseline mission is 2500 lb and is broken up between in situ instruments, fixed sensors and navigational equipment. Most of the equipment will be integrated into either the Qbay (aircraft's underside) or along the wings. Table 2.2 shows the weight and location on the aircraft of each piece of science hardware Sensors will be placed out on the wings where they are far enough away from any engine pollutants which would change the atmospheric data taken. Lines will be run into the Qbay, where the bulk of the science equipment and power sources will be situated. The whole air sampler along with several other instruments

will be situated in the engine booms.

Placing several of the instruments along the aircraft's wing will help with their cooling by integrating them with the cooling of the wing by using the aircraft's fuel (stored in the wings). The power required to operate the science instruments is 27 kW at a frequency of 400 Hz, 100 amps and 28 VDC. The power for the payload as well as the useful instrumentation will be bled off of the engine. Specifics of the scientific payload experiments will not be discussed here, as they are left for the NASA scientists to operate. All scientific instruments are of ER-2 inheritance, thus reducing cost quite significantly.

2.4 Telecommunication, Navigation and Data Handling

The aircraft's location at any time will be determined by utilizing overhead Global Position Satellites (GPS). GPS will allow the ground station to monitor the aircraft's position at all times within 1 ft of accuracy. To avoid using a chase plane and manual control at all times, the aircraft's flight path will be pre-programmed. In the case that the aircraft strays off course more than several hundred feet, as noted by the GPS tracking system, a manual override will be initiated putting the aircraft under the control of an operator on the ground station. Unfortunately, with the extreme range of the aircraft to an extreme geographic location, namely the South Pole, data acquisition will be a problem. The absence of ground stations and data relay satellites in the Polar regions require an alternate means of data acquisition and relay. High bandwidth, shortwave telecommunications will be implemented, backed with a pair of data record and playback systems for redundancy. The shortwave will allow for telecommunications over and around the horizon of the Earth, with the addition of the data recorders to record and store data at all times. Thus any loss in shortwave communication (due to solar or atmospheric interference) will not be a

failed mission. All data will be processed real time and backed, compared or replaced with that recorded on the aircraft's database.

Table 2.2: XR-1 Payload Distribution and Weights

Remote/System	Location	Weight (lbs)
Aerosol Particle Sampler	LH Wing	13
Microwave Temperature Profiler	LH Wing	67
Condensation Nucleus Counter	LH Wing	75
ClO/BrO Detector	Qbay*	304
Whole Air Sampler	LH Pod	138
Meteorological Measuring System	Qbay	93
Navigation (Intruments 1&2)	Qbay	140
Ozone Photometer #1	Qbay	124
H20 Vapor	Qbay*	114
H20 Total	Qbay*	120
NOx	Qbay*	352
Ozone Photometer #2	Qbay	74
Infrared/Solar Radiometers:		
Infrared Detectors	Qbay	74
Equipment	Qbay	136
Solar Detectors	RH Wing	10
Rack/Wiring	Qbay	74
Wing Scanner	RH Wing	43
Multi-filter Sampler	RH Wing	131
Particle Spectrometers	RH Pod	161
Atlas (CO/N2O)	Qbay*	281
TOTAL:		2500

* *Sensor feed to wing*

REFERENCES:

2.1 Anderson, John D.: Introduction to Flight, McGraw-Hill Book Company, New York, 1985.

2.2 Brune, Williiam H.: "Stratospheric Ozone and the Case Against Chloroflourocarbons," Earth and Mineral Sciences, November 4, 1989.

2.3 Fisher, David E.: Fire & Ice, Harper and Row, New York,1990.

2.4 Harber, Leonard C.: Causes and Effects of Changes in Stratospheric Ozone, National Academy Press, Washington D.C., 1984.

2.5 Hawkins, Frank H.: Human Factors in Flight, Gower Publishing Company, Brookfield, Ver mont, 1987.

2.6 Patrusky, Ben: "Dirtying the Infrared Window," Mosaic, Fall/Winter, 1988.

2.7 Roan, Sharon: Ozone Crisis, John Wiley and Sons Inc., New York, 1989.

2.8 Webb, Willis L.: Structure of the Stratosphere and Mesosphere, Academic Press Inc., New York, 1966.

2.9 Whitten, Robert C.: Ozone in the Free Atmosphere, Van Nostrand Reinhold Company, New York, 1985.

2.10 National Aeronautics and Space Administration: "Global Stratospheric Change," NASA Conference Publication 10041, Moffett Field, California, 1989.

2.11 National Aeronautics and Space Administration: "Very-High-Altitude Planform Aircraft Exploratory Studies," NASA Ames LetterSSG:245-5/136, Moffett Field, California, 1988.

3.0 Mission Design

Section Three deals with the creation of the mission profiles for the XR-1 HAMMER aircraft as well as an overview of the mission performance.

3.1 Mission Profiles Summary

Each of the four basic mission profiles will be discussed further in turn. Once again, note that the aircraft is not limited to only these mission descriptions. A wide array of missions may be flown within the limitations of the aircraft by changing such factors such as payload weight, fuel carried, and manned capability. The reference aircraft is an unmanned aircraft while shorter missions at less strenuous altitudes may implement a cockpit module for special manned missions. This would include any missions in which flight over populated landscape was required as well as short duration tests in which direct human control could improve the results obtained. Long duration flights such as those presented below, and flights over water, will best be satisfied with an unmanned aircraft. The argument of using either manned or unmanned aircraft will be presented in Section 3.1.5.

3.1.1 Baseline Mission Profile 1

Of all of the mission profiles examined, option 1 had the most stringent requirements and was thus used as the basis for the aircraft design. It was determined that if the aircraft could be designed to meet the mission 1 restraints, it would inherently be able to fly the remaining three missions as well.

Mission 1 (See Figure 3.1), also known as the baseline mission, begins with a takeoff from Punta Arenas, Chile (53° S). The aircraft will climb to a cruise altitude of 100,000 feet with a maximum climb speed at altitude of 600 fps. This provides a 20% margin over the stall speed. The aircraft will achieve the cruise altitude 700 n mi downrange of take-off after 2.5 hours of flight. The aircraft will cruise at 100,000 ft for 4800 n mi, including a semi circle turn over the South Pole and return to Chile, followed by a 500 n mi landing phase. The total mission duration is just under 16.0 hours with a total range of 6000 n mi. The XR-1 will carry the basic payload package weighing 2500 lb and will burn approximately 6800 lb of fuel. Gross take-off weight will be the standard 26,000 lb with a full fuel tank capacity.

The desired RFP payload weight of 2500 lb was met, as was the distance to climb to 100,000 ft (700 n mi). In order to meet aerodynamic and structural restraints and requirements, the takeoff weight was calculated to be 26,000 lb. This weight, along with the limitation of power output from the engine, limited the maximum rate of climb to an average of 12 fps. Using a scheme to reach the ceiling in the shortest distance allowed the aircraft to reach altitude within the RFP requirements, however, implementing the method of climbing with a minimum fuel requirement would take a longer distance on the order of an additional 150 n mi. Thus a compromise of

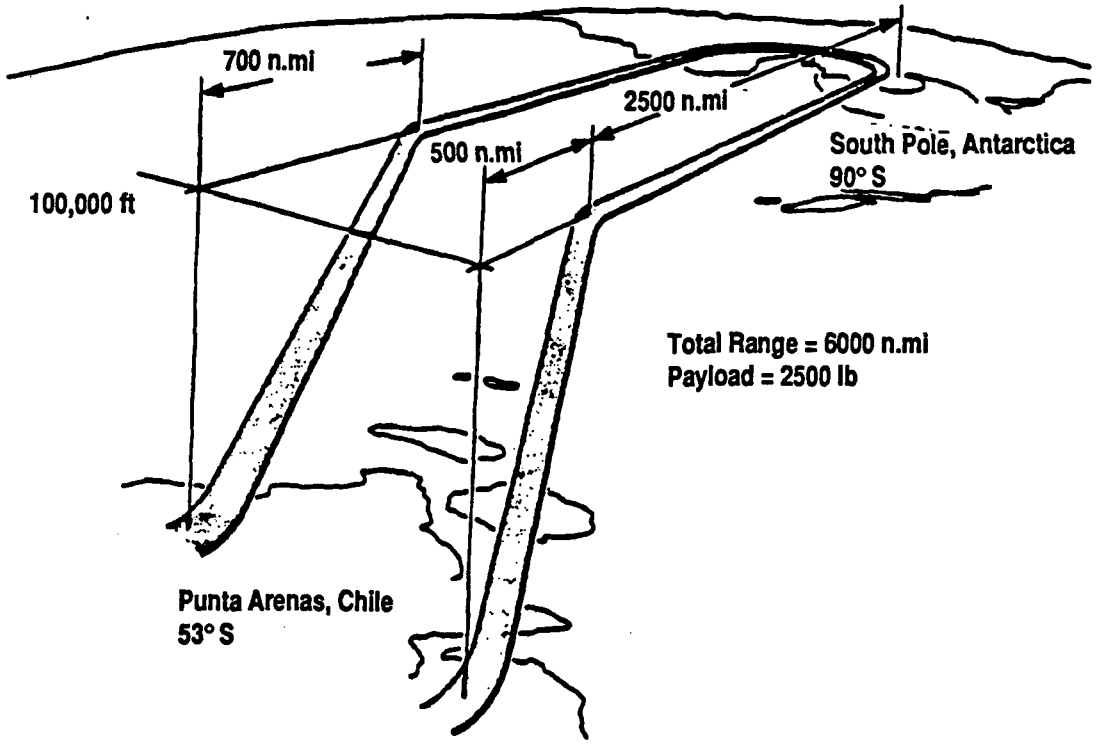

Figure 3.1: Polar Mission

burning the minimum fuel to attain the cruise altitude was used. The aircraft will be at altitude for 4800 n mi, allowing a large sample of quality data to be obtained throughout the mission duration, including at 100,000 ft in the region of the ozone hole over the South Pole.or the majority of the mission.

3.1.2 Reduced Altitude Mission Profile 2

Mission profile two is generally the same as mission 1 with two significant differences. The same flight path, Punta Atenas to South Pole to Punta Arenas, is flown for this mission (See Figure 3.2). However, this mission only requires a

maximum altitude of 70,000 feet, but also calls for an increased scientific payload above the standard 2500 lb package. Total time of flight is 17.5 hours with a time to climb of 1.5 hours. 6400 lb of fuel are burned and an enhanced payload of 4000 lb is available. Once again, the aircraft's gross weight will be 26,000 lb and fuel tanks will be completely full at take-off. The distance to climb for this lower altitude mission is 500 n mi and a landing phase distance of 300 n mi is also needed. The increased payload of 4000 lb and short flight time to altitude meets the RFP requirements. The extra 1500 lb in the science payload will be made available to the scientists as they may see fit.

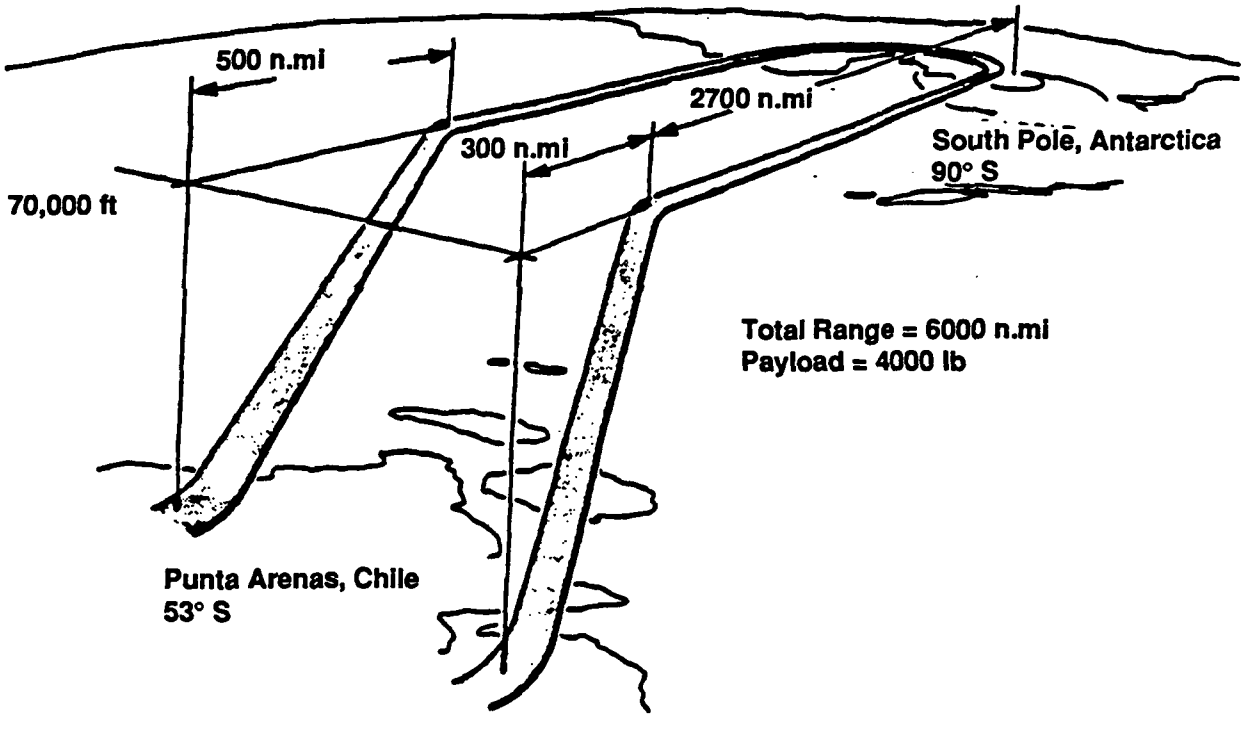

Figure 3.2: Polar Mission 2

3.1.3 Midlatitude Mission 3

The midlatitude mission is identical to the baseline mission profile with one exception. The XR-1 flight path will originate at NASA Ames Research Center, Moffettt Field, CA (37°N) and will continue on a straight path to Puerto Montt, Chile (41° S) (See Figure 3.3). This will allow sampling of the ozone at locations other than the polar region, namely the midlatitudes. All other aspects of this mission mimic that of the baseline mission (1) above.

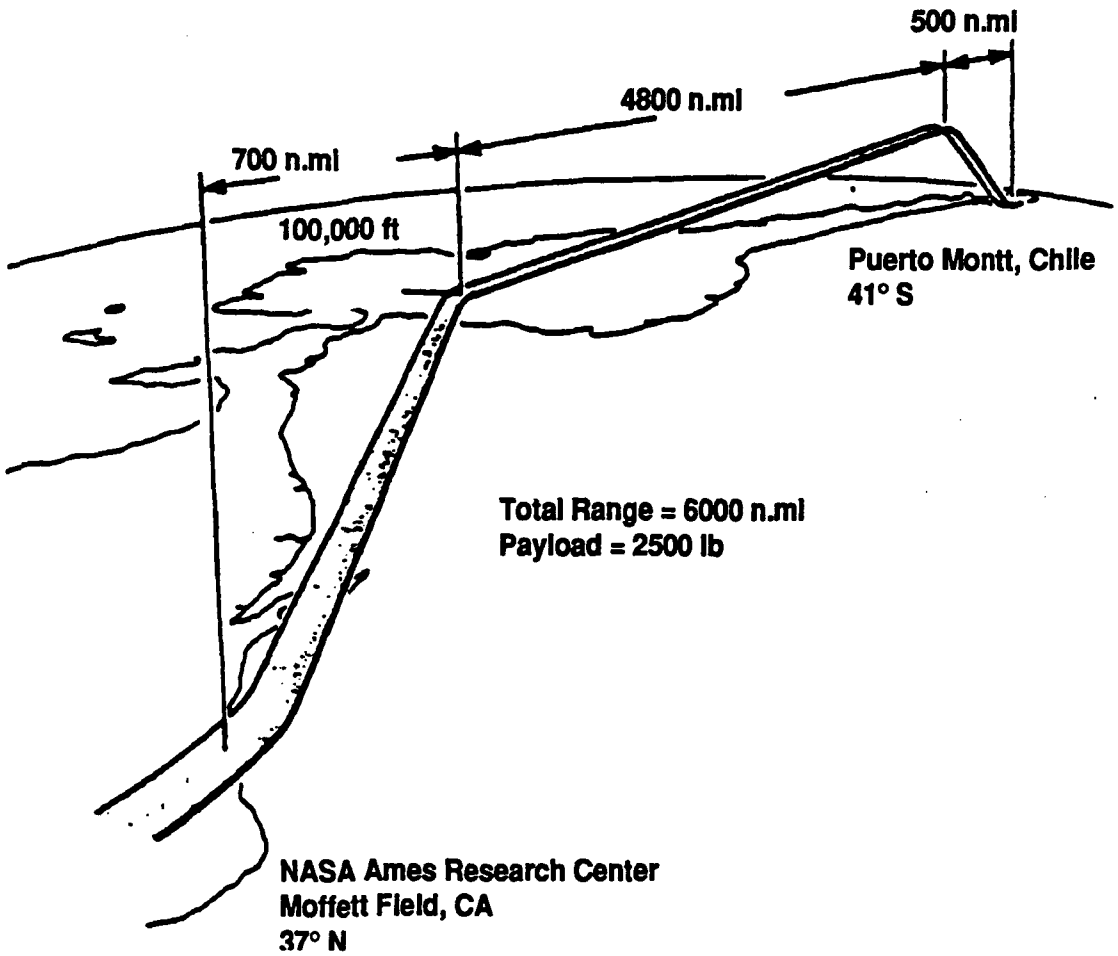

Figure 3.3: Midlatitude Mission 3

3.1.4 Midlatitude Zoom Mission 4

The final mission profile considered is a straight jaunt from NASA Ames Research Center, Moffett Field, CA (37°N) to Howard Air Force Base, Panama (8°N) (See Figure 3.4). This mission provides an added feature in its zoom up to altitudes above 100,000 ft. A zoom up to 120,000 ft was requested in the proposal. From energy and velocity methods, the maximum jump up altitude for the XR-1 is approximately 111,000 ft. Altitudes of 120,000ft were unattainable due to the exponential drop in density, engine power limitations, and cooling restraints. However, even this momentary zoom will allow the science team the possibility of learning even more about the ozone gradient with altitude. This zoom may only be obtained at a point where the aircraft's wet weight falls below 20,000 lb and only under full throttle, occuring towards the end of the mission just prior to the landing phase. No exteneded period of endurance at this altitude will be possible other than the mere zoom up, followed immediately by the landing phase. If large head winds cause an excess of fuel to be burned, the XR-1 program's exectutive test officer (PETO) will be responsible for any decision with proceeding with the zoom. The mission range is cut to 3250 n mi with a time of flight of under 9 hours and a time to climb to 100,000 ft of 1.4 hr. This reduced range requires less fuel, (3500 lb) and, due to the excessive altitude reached during the zoom up, a payload trimmed to 1000 lb. These lower payload and fuel requirements allow a partially filled tank and thus a lower gross take-off weight for this particular mission. The aircraft's gross weight will be 22,000 lb for the zoom mission. It is also interesting to note that an additional 800 lb are available for increased payload, or even for a possible manned mission module. The shorter flight duration (9 hr) makes this a candidate for a manned

mission, which may be preferred since the aircraft will be flying over populated Latin America (See Section 3.1.5).

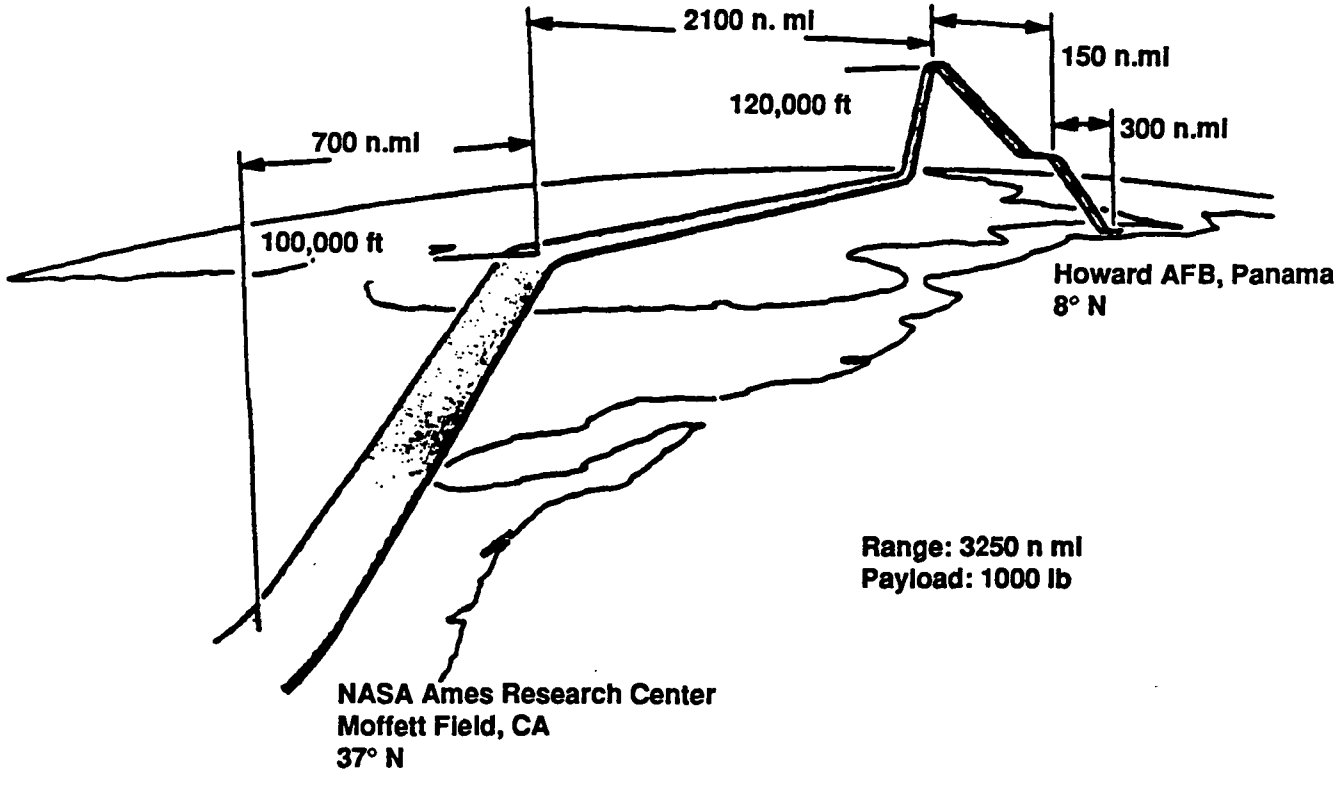

Figure 3.4: Zoom Mission 4

3.1.5 Manned Vs. Unmanned Flight

Several justifications may be made for both manned and unmanned flight in the XR-1. Manned flight would be preferred since the pilot would be able to more closely monitor the aircraft rather than relying on data links for every desired action. Of course, this will increase the aircraft's weight and decrease its simplicity by adding the pilot and his life support system. It will also drive up the cost of the aircraft with

its more difficult design. On the other hand, Congress is probably more likely to support an aircraft that is manned due to the nature of the mission and the hazards that may be involved, not to mention their concern of an unrecoverable loss due to a malfunction of telemetry. Manned flight also lessens the restrictions on airspace, allowing the aircraft to fly over more land and populated area, thus covering more of the earth. Unfortunately, pilots are human and will not fair too well sitting motionless in a tiny cockpit while wearing an uncomfortable full pressure suit for a mission duration of over 16 hours. It is for exactly this reason, along with the weight constraints, that the unmanned design was adopted. It is however feasible to implement a human module interface into a production aircraft, allowing for manned flight in shorter duration flights (which require less fuel) as well as special purpose flights and flights over populated regions. This manned module would be located above the Q-Bay of the aircraft. This location reduces pilot visibility, but since the aircraft is capable of flight autonomously this should not be a problem.

3.2 Aircraft Performance Analysis

The XR-1 HAMMER performance analysis may be divided into four primary segments: Take-off, Climb, Cruise and Landing. Each segment will be looked at in turn. The performance discussion below is applied to the most stringent aircraft mission (Baseline Mission 1) of 6000 n mi range at 100,000 ft.

3.2.1 Takeoff Phase

The XR-1's gross weight is 26,000 lb upon engine start. This includes a dry structures weight of 11000 lb, three engines for a total of 5700 lb, payload of 2500 lb, and 6800 lb of fuel. It is assumed that an amount of fuel equal to 1% of the aircrafts

total weight will burn during the takeoff phase (260 lb). This leaves a gross takeoff weight of 25,740 lb at liftoff. A takeoff speed of 75 fps and a distance of 3800 ft will be required on a static day. Any winds in excess of 20 knots could require a mission delay, especially for direct crosswinds. The PETO will be responsible for giving the green light at the scheduled mission time. Under safe conditions, a takeoff roll distance of no more than 1000 ft will be required. The runway width of 60-75 ft will be able to support the aircraft which has a maximum gear to gear width of 50 ft. The wind tips will be capable to clear off runway obstacles of at least 4 feet with the 232 ft wingspan.

3.2.2 Climb Phase

The climb phase will take the aircraft from sea level to 100,000 ft, the cruise altitude. An average climb angle of 1.2° (R/C=12 fps) will bring the aircraft to maximum altitude 700 n mi down range of the airstrip. The aircraft will end the climb phase at 600 fps. Original plans accounted for aerial refueling once the aircraft reached an altitude of 30,000 ft. This would allow a 1200 lb reduction in fuel weight and therefore a 1200 lb increase in the aircraft's dry weight. However, due to advances that reduced the airplane's drag, thereby increasing its glide ratio, the aircraft was able to operate without the necessity of refueling. If future revisions cause a significant change in the required weights, this alternative will still be avialable. According to the energy method calculations as presented in the XR-1's flight profile, the fuel consumption pattern nearly represents the minimum fuel comsumed to reach 100,000 ft. at a speed capable of meeting RFP requirements as mentioned in section 3.1 above. Once cruise altitude is reached, the aircraft is throttled back to achieve a cruise speed of 650 fps. The power profile for the XR-1

is illustrated in figure 3.5. It is seen that the power will increase as the altitude increases (density decreases) and will max out at 1350 hp at 100,000 at which time the aircraft is throttled down to about 900 hp for the cruise phase. As fuel continues to burn, less power is required and the engines will be run slower still. Figure 3.6 represents the flight envelope for the XR-1. The aircraft is limited by the stall Mach number on the lower side and by the maximum power output Mach number on the higher scale. On the right side, the XR-1 is also limited to a maximum Mach number of .65. Cruise at higher altitudes (to 111,000 ft) is possible if flight at higher speeds is allowable.

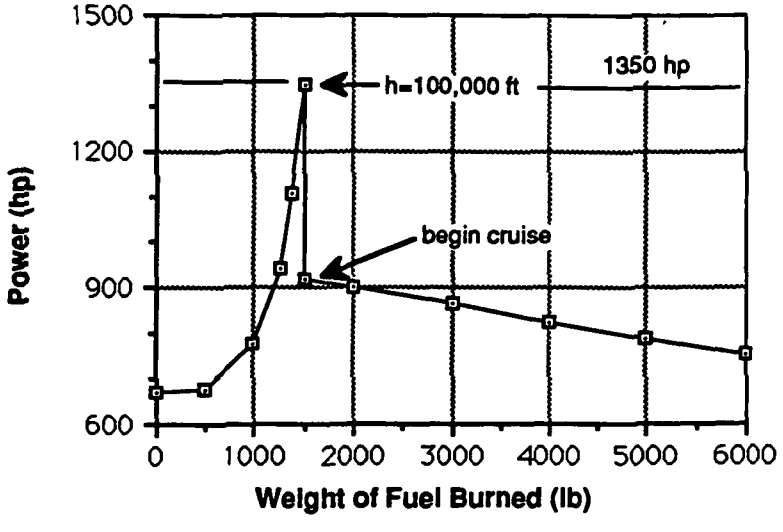

Figure 3.5 :XR-1 Power Required Profile for Baseline Mission

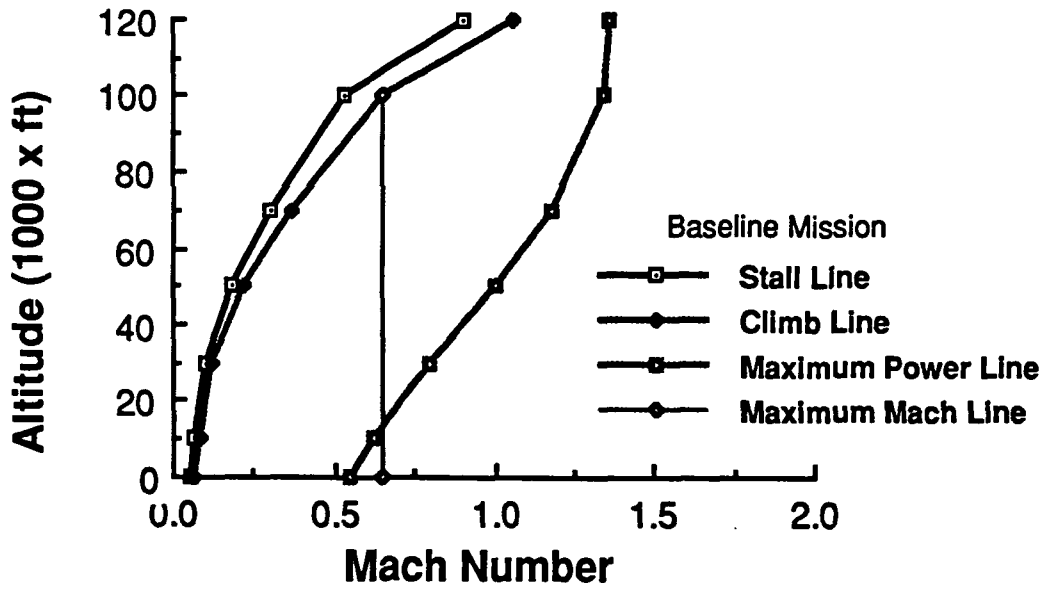

Figure 3.6: XR-1 Flight Envelope

3.2.3 Cruise Phase

The cruise phase consists of the bulk of the high altitude mission. It is at this altitude that all scientific data will be taken, although sampling will begin at takeoff. As previously mentioned, a mission of 6000 n mi is required with 4800 n mi at the 100,000 ft cruise altitude. Calculations resulting from the Breguet range equations allow for a mission in excess of the required range. The aircraft will cruise at no more than 650 fps depending on the power required at a particular mission time (See Figure 3.5). As the fuel burns off, less power will be required to keep the aircraft's lift in excess of its drag. Keeping the engines throttled back will result in a greater fuel savings for the mission duration, thus allowing a larger dry aircraft weight. For mission 4, a zoom up to 120,000 ft is desired, though 111,000 ft is attainable. Once

the aircraft is 2800 n mi down range, enough kinetic energy is available to convert into a boost up to 111,000 ft in altitude. Once the aircraft reaches this upper limit, it will begin its landing sequence.

3.2.4 Landing Phase

The landing phase will begin 500 n mi (300 for mission 4) short of the landing strip, at an average rate of descent of 17.3 fps (25 fps) The velocity will be 550 fps at the beginning of the departure from cruise and will need to be approximately 70 fps upon touchdown. A landing distance of 3000 ft will be required. In order to descend with the huge amounts of lift the aircraft will be producing, spoilers will be engaged to dump the excess lift. Enough reserve fuel will exist for the aircraft to safely reach the landing strip regardless of a strong headwind which could slow the aircraft down and require an expenditure of more fuel that originally expected. Also, with the L/D ratio of 35, the aircraft is capable of gliding in for virtually the whole landing sequence. At touchdown, the aircraft will weigh approximately 19,000 lb (for the baseline mission).

3.3 Mission RFP Requirements

Table 3.1 summarizes the mission profiles for the XR-1. In compariosn to the RFP, all range, altitude, climb distances, and payload weights were met with one exception. As mentioned previously, the maximum altitude for the zoom mission (Mission 4) is 11,000 ft, 9000 ft of the desired altitude. This extende 11,000 ft will also allow a better understanding of the ozone layer's structure at the extende altitudes. All payload weights, ranges, and all other maximum altitudes as well as distances

to climb as shown in the preceding mission profile diagrams, correspond to the RFP requirements.

Table 3.1: Mission Profile Summary

MISSION	I	II	III	IV
Range (n mi)	6000	6000	6000	3250
Max Altitude (ft)	100,000	70,000	100,000	110,000
Time of Flight (hr)	16.0	17.5	16.0	9.0
Time to Climb (hr)	2.5	1.5	2.5	2.5
Fuel Weight (lb)	6800	6400	6800	3500
Payload Weight (lb)	2500	4000	2500	1000

4.0 – AIRCRAFT DESIGN

4.1 Configuration

Hundreds of possible aircraft configurations may be considered in the design selection. For this discussion, only the more feasible configurations were analyzed, and are listed below. Each possible configuration will be discussed in turn.

1. Conventional
2. Flying wing
3. Joined wing
4. Standard with Canard
5. Biplane
6. Twin–Fuselage
7. Tandem wing

4.1.1 Conventional

Conventional aircraft configurations have dominated the realm of design, but

in the past ten years new innovations have emerged. A conventional configuration aircraft is simply a single fuselage, with a single wing and conventional tail properly attached. This type of configuration is shown in Figure 4.1:

The generation of lift created by the wing is directly related to the atmospheric density, wing area, wing lift efficiency factor (CL), and velocity. To obtain the maximum lift, a variety of methods may be utilized. These include decreasing the aircraft weight, increasing the wing area, or increasing the wing lift coefficient. The maximum Mach number which can be obtained without suffering the effect of Mach buffet is approximately 0.7. Selecting the appropriate airfoil will optimize this speed in terms of aerodynamic efficiencies. This, in essence, results in a higher wing lift coefficient. If the wing area is enlarged, however, a penalty occurs in the form of added structural weight. This result causes a decrease in the aerodynamic efficiency. Thus, trade-offs are required.

The conventional aircraft which will meet the RFP requirements must have an extremely large wingspan. Due to this requirement, large bending moments introduce structural difficulties and, as a result of the large wing deflections, aerodynamic deterioration occurs in the form of loss in lift.

The conventional aircraft will also have problems with ground clearance. The propeller, which is mounted onto the engine shaft, has a maximum diameter of 20 feet. Since the length is abnormally large, special consideration must be given to its placement on the aircraft. The XR-1 must have large diameter propeller in order to increase the propeller power. On the other hand, this configuration will be more stable due to its familiarity in aviation. A conventional aircraft can easily be modeled on computers and could be build with current technology.

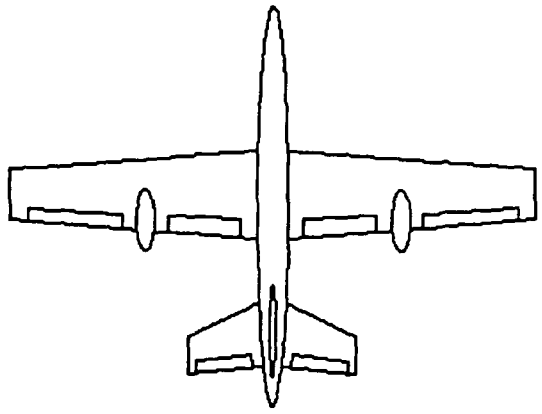

Figure 4.1: Conventional Aircraft Configuration

4.1.3 Joined Wing

The joined wing was also considered because of its unique and relatively innovative concept. This type of aircraft would have a lighter structural weight due to its vertical bracing, however, its aerodynamic efficiency is questionable due to the increased drag. This is caused by mutual interference effects between lifting surfaces and intersections. A joined wing configuration is shown in Figure 4.3 :

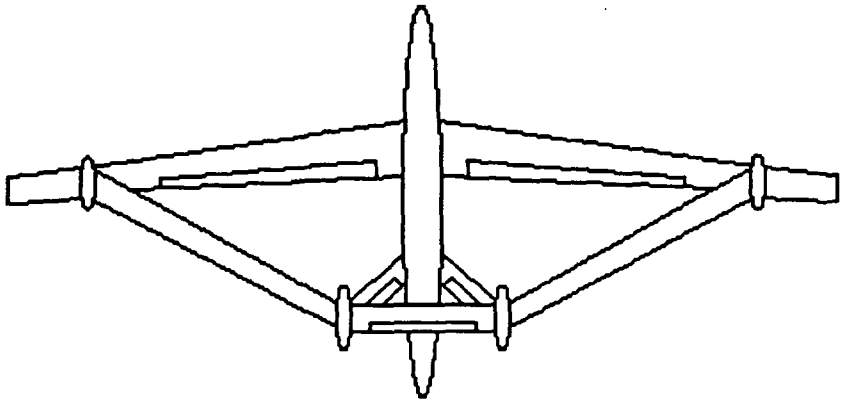

Figure 4.3: Joined Wing Configuration

An advantage of the joined wing is the unique combination of an anhedral and dihedral wing attachment which provides good lateral stability characteristics. Since these two wings are joined together, the aircraft is extremely strong in terms of its structural strength and rigidity. This strength is an especially desired quality for aircraft with large wing spans. Having the wings joined at the 70% span position the maximum structural efficiency is obtained. One problem that was encountered with the joined wing configuration was that it was not a proven technology. In other words, there were no existing joined wing aircraft that could be used as examples to show how well the idea works in actuality. For this type of configuration the propeller clearance does not represent a problem since the large propellers could be mounted at the intersection of the aft wing and the vertical tails. Advantages claimed for the joined wing are:

1. Light structural weight
2. High stiffness
3. Low induced drag
4. Good transonic area distribution
5. High trimmed CL max
6. Reduced wetted area and parasite drag
7. Direct lift control capability
8. Direct side force control capability

Joined wings are not invariably lighter than aerodynamically equivalent

conventional wing–plus–tail systems. Weight will be saved only if the geometric parameters of the joined wing such as sweep, dihedral, taper ratio, and joint location (as a fraction of the span) are properly chosen. In addition, the internal wing structure must be optimized, with the wing box occupying the section of the airfoil between 5 and 75% chord (or greater if possible).

4.1.4 Canard

The canard also has an even lower lift-to-drag ratio than the conventional design. It would have some stability problems if maximum efficiency is the primary goal. Utilizing a canard does not significantly minimize the structural weight. The main redeeming quality of the canard configuration is that at higher angles of attack, the canard stalls first which prevents the aft wing, where most of the lift is produced, from stalling. If the engines are mounted on the wing as pusher propellers to retain maximum flow over the wing, the propellers may hit the ground at takeoff or landing due to the takeoff rotation. Another advantage of the canard configuration is the reduced trim drag. A canard configuration is shown in Figure 4.4 :

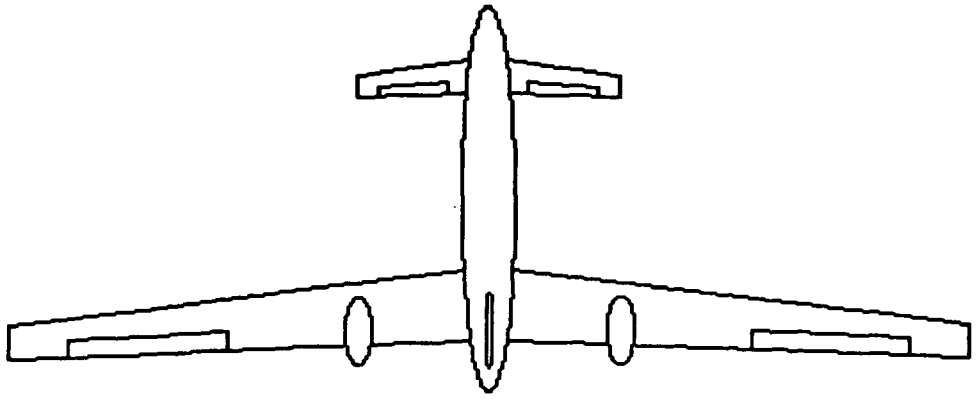

Figure 4.4: Canard Aircraft Configuration

4.1.5 Biplane

Biplane technology saw its heyday during the early days of aviation, after which, until recently, has been all but forgotten. Now this type of technology has resurfaced. The biplane configuration can yield a lower induced drag if the wings are correctly staggered and spaced. Since there are two wings, the amount of lift that is required may be distributed between those two lifting surfaces. The biplane would thus have a shorter wingspan than the conventional aircraft while generating the same amount of lift. By mounting the engines on the top wing, the propeller clearance problem is alleviated. One problem that does exist with the biplane is the interference effect from the wing struts. This results in large values for interferece drag, which, at higher altitudes, could exceed the available power. Even though the overall wingspan would be reduced through the use of dual wings, the span must still be quite large. The bending moments in high aspect ratio wings result in the need for long struts to support the wings, this implies an additional increase in drag. The biplane configuration is shown in Figure 4.5:

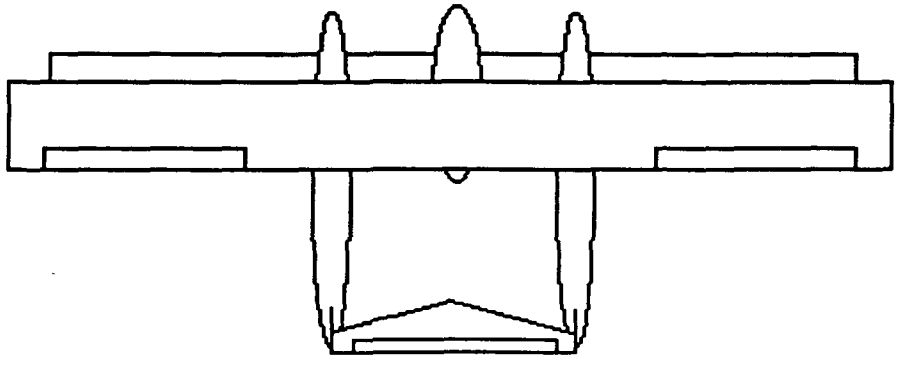

Figure 4.5: Biplane Aircraft Configuration

4.1.6 Twin Fuselage

The twin fuselage concept featured dual fuselages with space for large phased–array synthetic aperture radars (SAR), providing increased detection capability. In addition to distributing fuel along the wing, increasing the distance between the fuselages further reduced wing bending moments and, hence, wing structural weight. Incorporation of fuselage–mounted engines and the use of large diameter propellers required four long landing gear or a separate ground support "carriage" for takeoff. With the large diameter propellers, landing was also a problem. Both of these approaches were undesirable from a logistic or operational point of view. Twin fuselage aircraft yield up to a 40% decrease in fuel consumption. Twin fuselage configurations also offer the advantage of being able to utilize high aspect ratio wings without structural and/or weight penalties. . Working with aspect ratios greater than 10 is a relatively new area since, for several years, the practical upper limit for the aspect ratio of an aircraft was set at a value of (approximately) eight.

4.1.7 Twin Boom

The twin boom configuration was designed for a higher wing loading at cruise conditions at the cost of a lower stall margin during cruise. The effect of having twin booms is similar to that of the twin fuselage design. The twin booms were used to provide structural strength to the large horizontal tail and space for landing gear retraction. The twin boom/twin fuselage configuration is shown in Figure 4.6 :

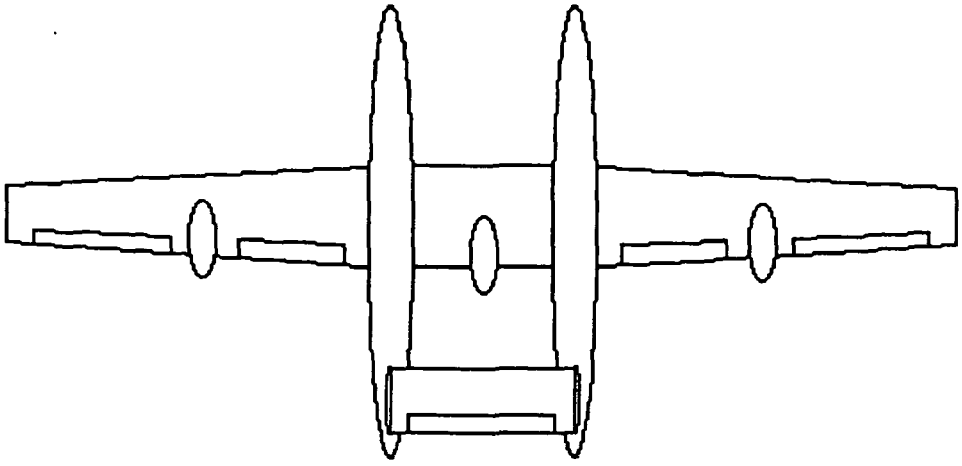

Figure 4.6: Twin Boom/Twin Fuselage Aircraft Configurations

4.1.8 Tandem Wing

The front wing, which angles up slightly more than the rear one, doubles as a canard. The rear wing extends farther out on either side. Both wings have slender, high aspect ratio shapes, similar to those of gliders, that provide good long–range flying efficiency. However, the high aspect ratio airfoils pose a problem: slender wings are not very strong when twisted. Therefore, in order to support the loads from the fuel, engines, and landing gear, the wings obtain structural support from the booms that connect them. Then the loads from the landing gear and the engine become bending loads rather than twisting loads. Giving the forward wing a slight positive angle of attack makes it stall before the rear wing, similar to a canard. Since the aircraft has tractor propellers instead of pusher propellers, the pod, or boom, behind the engine was lengthened to reduce drag.

The tandem wing/twin boom design promises a low structural weight. Due

to the fact that the span–loading concept of distributing the weight of the aircraft along the wing minimizes bending moments on the wing, a reduction in structural weight results. Proof of this was the Rutan Voyager aircraft. The resulting structural weight was 9.7% of the total aircraft weight, compared with about 25% for a conventional aircraft configuration. Another advantage of the tandem wing/twin boom design is that high aspect ratios can be acquired for a shorter span length than a single wing would require for the same aspect ratio and surface area. A disadvantage for this type of configuration is the interference drag that is accumulated from all the surfaces. Some of the tandem wing/twin boom configuration advantages are: :

1. Light structural weight
2. Moderate to high wing stiffness
3. Low induced drag
4. High trimmed CL max
5. High combined aspect ratio
6. Forward wing prevents aft wing from stalling
7. Landing gear can be stored inside booms
8. Reduced span for same surface area
9. Lower bending moments from the wings

With these crtieria in mind, it was possible to compare the different configurations and make an informed decision on the proper configuration for the HAMMER.

4.2 Configuration Finalists

The twin boom configuration (as shown previously in Figure 4.6) seemed promising because of its structural characteristics. The two booms and the center cabin would provide a favorable combination for the distribution of bending moments due to wing loads. However, according to the mission constraints (maintain a cruise altitude of 100,000 ft) the wing had to have a relatively large span in order to maintain favorable aerodynamic characteristics. In addition, this configuration could not accommodate a third engine easily, should it be necessary to overcome the drag created by the aircraft.

The alternate configuration that was proposed at the beginning of the design process, was that of a tandem wing airplane (Figure 4.8).

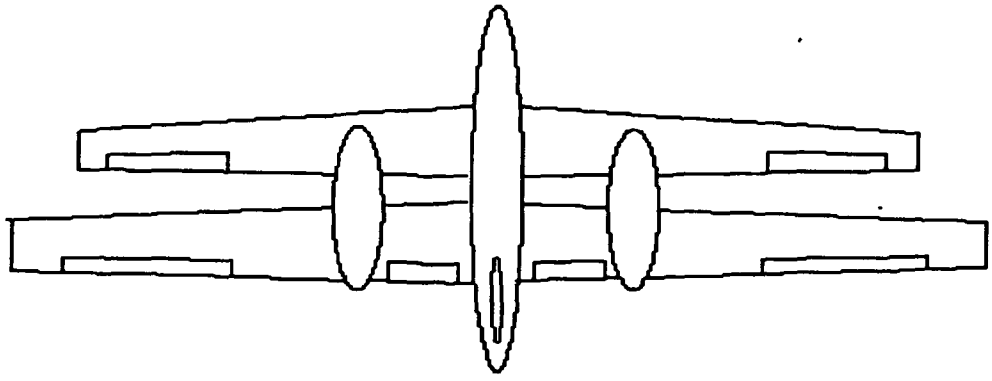

Figure 4.8: Tandem Wing Configuration

The tandem wing configuration presents the clear advantage of dividing the lifting surface into two smaller wing surfaces, thereby eliminating the excessive span required by the twin boom configuration. Initially, there was some concern that the tandem wing configuration would produce more drag than the design could afford;

nonetheless, it was found that certain modifications would reduce the drag.

Interference between the two wings due to the effects of upwash and downwash, was another problem that would be encountered in the implementation of a tandem wing. However, such interference could be minimized by adjusting the incidence of the wings, such that the flow impinging on the wing produces an effective angle of attack close to zero.

With the concerns mentioned above, the tandem wing configuration was modified to solve those problems. A third engine was added in the nose for increased power and aircraft safety. Another modification made to simplify the construction of the aircraft was the elimination of the horizontal tail. This could be justified through the use of the forward wing acting as a canard to serve as a horizontal stabilizer.

Section 4.3 discusses in detail, the geometric characteristics of the final tandem wing configuration.

4.3 Final Configuration

The configuration of HAMMER is basically that of a single fuselage, tandem wing aircraft featuring only a vertical tail (v. tail) in the empennage. The aircraft is to be powered by three engines, two of which are attached to the wings, and the one located in the nose of airplane. The forward–most wing (fore-wing) has a dihedral and the second wing (aft-wing) has an anhedral; both of the wings are moderately swept–back. Figure 4.9 is a three-view drawing of the aircraft.

1.

FOLDOUT FRAME

2.

FOLDOUT FRAME

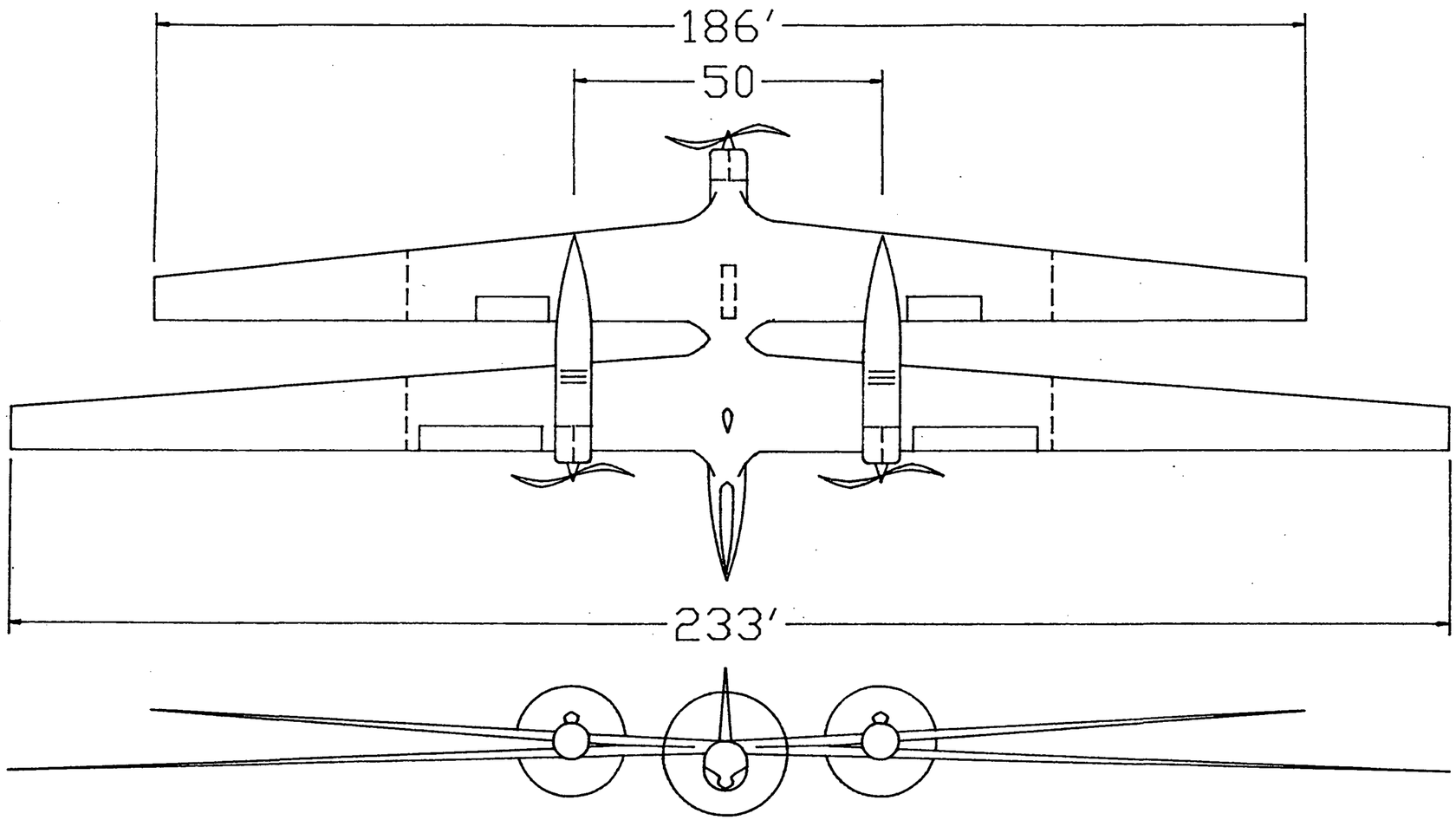

XR-1 HAMMER
NASA/USRA
CAL POLY, POMONA

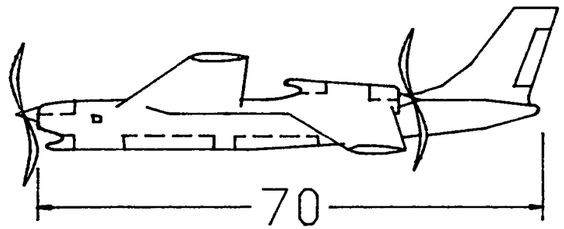

Table 4.1: Aircraft Geometric Parameters:

Paramete	Aft Wing	Fore Wing	V. Tail
Span, b	233 ft	186	26
Root chord, Cr	16 ft	17.1	10
Tip chord, Ct	7.2 ft	7.6	4.5
Taper ratio	0.45	0.44	0.28
Reference area	2703 ft^2	2297	533
dihedral	-5 deg.	4	0
LE sweep	5 deg	6	60
Aspect ratio	20.1	15.1	1.3

Other Parameters	
Fuselage length	70 ft
Fuselage average diameter	5.7 ft
fuselage widest diameter	6.6 ft
wing separation (root)	9.0 ft
y-location of wing engine	22 ft
location of A.C.	39.3 ft
location of C.G.	34.2 ft

This configuration was chosen over the others presented in Section 4.1, because it provides the necessary lifting area demanded by the missions requirements. Two wings were chosen instead of a single wing in order to achieve the desired lifting area, with less structural and weight penalties. Since the first wing provides canard effects that facilitate static stability, it was found that no horizontal tail was necessary if the wings were positioned with that in mind. The engine shrouds are also bracing structures that aid in the distribution of the bending moments created by the wings. The moderate size of the vertical tail is an indication that a stability augmentation system to enhance lateral stability will be implemented.

The proposed configuration was chosen based on the design flight characteristics corresponding to the beginning of the phase of cruise, at an altitude of 100,000 ft, a speed of Mach 0.65 (or 381 knots), at which time the aircraft will have a weight of approximately 24,500 lb. The wing loading will then be of 5.1 lb/(ft^2).

4.4 Mission System Requirements

The various missions capabilities required for this aircraft, in general, are: cruise altitude for ozone sampling between 70,000 ft. and 100,000 ft. with one excursion to an altitude of 120,000 ft., the missions range between 3,250 and 6,000 nautical miles.

The identifiably systems required to comply with the mission requirements and maintain a viable aircraft are the following:

- Telemetry Systems
- Power System
- Stability Augmentation Systems
- Fuel System
- Heat Dissipation/Anti–icing System
- Data Acquisition Systems
- Instrument Landing Systems
- Land Support Systems

4.4.1 Telemetry Systems

The telemetry system in the aircraft will have a dual role: to provide data management linkage between the Data Acquisition System and the corresponding Land Support sub–system; at the same time,the telemetry system is to support flight control by acting as a bridge between the on–board flight subsystems, the Stability Augmentation Systems and the corresponding Land Support sub–system.

4.4.2 Power System

As its name indicates, the job of the power system is to manage the performance of the engines in response to the needs of each mission phase, or other preplanned or eventual circumstance, that will necessitate variations in power output of the engines. The details of this system depend on the specification of the engines used.

4.4.3 Stability Augmentation Systems

The stability characteristics of the aircraft are such that, although the aircraft is inherently stable in its longitudinal modes of motion, it is unstable in the lateral modes of motion. As a result, the use of a stability augmentation systems (SAS) is inevitable, particularly in this case where the aircraft is to be unmanned.

4.4.4 Fuel System

The fuel is to be stored exclusively in the wings to facilitate its transfer to the

engines, and its circulation for engine cooling, and to better manage the travel of the center of gravity of the aircraft. For the main fuel stores, integral tanks are proposed and implementation of a porous foam material in the tanks is recommended; integral tanks provide better utilization of the wing internal volume, and the porous material reduces fire hazards by preventing fuel leakage from the tanks, with only a 3% volume loss versus a 10% penalty if bladder tanks were to be used. Integral tanks also have weight advantages with respect to the alternative bladder tanks.

4.4.5 Heat Dissipation/Anti–Icing Systems

The cruise altitudes required from the aircraft place a clear burden on the engines, in terms of the difficulties of heat dissipation due to the low air density at such altitudes. As a result, active mechanism for heat dissipation are a must. The heat dissipation system will also serve as an anti–icing system.

4.4.6 Data Acquisition System

The data acquisition system is comprised of the instrumentation destined for the sampling of air, and for the determination of flight conditions (i.e. air static pressure, flight speed, etc.). The data is to be "fed" to the Telemetry System for relay to the Land Support Systems. The location of the scientific instruments, for the sampling of air, is desired in a location where the air properties are largely undisturbed, and where the desired location of the center of gravity of the aircraft will be benefitted.

4.4.7 Land Support Systems

The Land Support Systems is, in reality, a conglomerate of subsystems. The functions of those subsystems are: to implement the ground logistics in preparation for a successful mission; to maintain flight control of the aircraft, at all times; to acquire and process data received from the aircraft; to revise the acquisition of data if necessary; and to maintain air logistics during flight and upon the landing phase

4.5 Weight Estimation

In order to have a starting point, an initial weight estimation was done. The method used was presented in Reference 4.7. A spread sheet using Lotus 123 was created in order to determine the initial weight sizing. This spread sheet is listed the Appendix. This utilizes uses the weight fraction method and this method is supported by different types of aircraft trends. This method is also dependent on the aircraft missions, and payload. Having all this considerations in mind the results were:

Table 4.2: Preliminary Weight Estimation

	Aluminum	Composite
Takeoff Weight (lb)	33,830	26,000
Fuel Weight (lb)	10,470	6,800
Empty Weight (lb)	15,160	11,000
Payload Weight (lb)	2,500	2,500
Propulsion Weight (lb)	5,700	5,700

As the range of the mission increases so does the takeoff gross weight, similarly as the payload increases the takeoff gross weight will increase linearly. For this reason, the preliminary weight estimation uses the maximum payload and maximum range mission, namely, Mission 1.

For the final weight estimation an average between Reference 4.7 and Reference 4.10 was used. The Cargo/Transport and the subsonic aircraft equations were used, since these categories are the ones that must closely approximate our aircraft the most. Having this in mind the results are listed on Table 4.3:

Table 4.3: Component Weight Breakdown

Component	Weight (lb)
Forward Wing	2870
Aft Wing	4125
Vertical Wing	450
Fuselage	520
Booms (2)	700
Landing Gear	850
Fixed Equipment	1485
Engines	5700
Payload	2500
Fuel	6800
TOTAL	26,000

4.1 Baullinger, N.: "High Altitude Long Endurance (HALE) RPV", AIAA Paper # 89-2014. August 1989.

4.2 Bollinger, B.: "High Altitude Atmospheric Research Platform (HAARP) Development", Lockheed Company, 1990.

4.3 Houbolt, John C.: "Why Twin-Fuselage Aircraft?", Astronautics and Aeronautics. April 1982.

4.4 Kirschner, Edwin J.: Aerospace Balloons. Aero Publisher Inc., Fallbrook, California, 1985.

4.5 National Aeronautics and Space Administration: "Very-High-Altitude Planform Aircraft Exploratory Studies", NASA Ames Letter SSG: 245-5/136. Moffett Field, California, 1988.

4.6 Poladian, D. and D. J. Reinhard: "High Altitude Reconnaissance Aircraft Design", AIAA Paper # 89-2109. August 1989.

4.7 Raymer, Daniel P.: Aircraft Design: A Conceptual Approach. American Institute of Aeronautics and Astronautics, Inc., Washington D.C., 1989.

4.8 Riedler, W.: Scientific Ballooning. Pergamon Press, Inc., New York, 1979.

4.9 Wolkovitch, J.: "The Joined Wing: An Overview", AIAA Paper # 85-0274. January, 1985.

5.0 System Functional Descriptions

5.1 Aerodynamics

5.1.1 Airfoil Analysis

Since the RFP requires the XR-1 to maintain flight at altitudes of 100,000 feet, the Reynolds number for the aircraft was considered. According to standard atmospheric tables, the density of air is 74 times less than that at sea level. Based on this information, a study was conducted to determine the most beneficial and appropriate region of Reynolds numbers to permit a successful mission.

Re is defined as the ratio of inertial forces to viscous forces. In short the lower the Re value, the more viscous the fluid becomes along the wing's surface. For the XR-1's mission profile, viscosity is the key element to obtaining feasible aerodynamic parameters. As stated previously, the air is much less dense at the chosen altitude; therefore to generate sufficient lift the flow must somehow remain attached to the wing surface. Ideally a turbulent flow is desired. In context, a typical Re for subsonic transports at altitudes of 40,000 feet is approximately six to nine million. For an aircraft which possesses a similar mission profile as the XR-1,a Re of 500,000 or 600,000 is more realistic. The Condor reconnaissance vehicle, designed by Boeing,

possesses a Re of 550,000 and can match altitudes to 70,000 feet. Based on this information, a good starting point for survey would be Reynolds numbers equal to and below 1,000,000.

5.1.2 Reynolds Number

This parameter was investigated and applied to airfoils specialized for this low Reynolds number regime as well as the typical NACA airfoils for subsonic flight. To determine an appropriate range, a process of elimination was desired. Through this method, regions of Reynolds numbers would be dropped from the survey. Also, a condensed selection of airfoils would be available to choose from as a result of the Re elimination. Selected airfoils were analyzed including the NACA six series, the specialized low Re LRN(1)-1007, the Lissaman 7769, as well as some Liebeck and Eppler series. Investigation also was established for boundary layer apparat such as transitional and separation control. Studies from these pieces revealed a well defined understanding of the range of Re desired as well as which airfoil suited the purposes of flight. Also, the necessity of whether or not any boundary layer assistance was needed to aid in maintaining a high lift coefficient was determined.

The first elimination sequence was determined through a phenomena known as hysteresis. This is an occurrence which some airfoil exhibit near stall and the strength of the aerodynamic forces, such as lift and drag, of that particular airfoil depends on the direction of the change in angle of attack. At stall, an abrupt decrease in lift and a significant increase in drag occurs. Some of the Liebeck airfoils at a Re above 700,000 exhibited this characteristic as well as the NACA 63-018. As a matter of fact, most NACA airfoils researched experienced hysteresis in one form or another at varying Re. The only alternative to inhibit these occurrences was to forcibly induce

a boundary layer tripping device on the airfoil which would immediately cause a turbulent boundary layer to form. In this manner, the turbulent flow would have a higher energy content to keep itself attached to the flow. However, since the flow is already unstable, this action would only maintain a high pressure distribution for a small range of angles of attack. Due to the inconsistency of these airfoils and the methods needed to maintain high lift coefficients, the NACA series were thrown out.

The other extreme was then researched for a possible Re range, and values between zero and 500,000 were studied. A region of undesirable effects were discovered for Re below 350,000. These effects, called separation bubbles generated a loss of lift and significant increase in drag characteristics. Some airfoils which were tested at much lower values, such as 50,000 to 100,000, could not even attain a marginally acceptable pressure distribution unless some type of boundary layer tripping device was associated with them. The LRN(1)-1007 (ref 5.49) was tested for a chord Re of 100,000 with an acoustical excitation device attached to it. This airfoil exhibited phenomenal results. Laminar flow existed for nearly 70% of the chord length at an angle of attack of eight degrees. At AOA of 18 degrees, a lift coefficient was generated at a value of nearly 1.60. The results of this airfoil was not uncommon to those which possessed this acoustical excitation device. In essence, sound waves generated from a nearby source would cause the laminar boundary layer to remain attached to the airfoil surface causing minimal amounts of drag. Unfortunately, the reasons which cause this tripping device to be so prominent is still uncertain and extensive testing is further needed. As a result, the airfoils which generated these results were useless for the time being and the Reynolds numbers below 350,000 were discarded.

It appeared that the only range which was acceptable for the mission profile were value between 400,000 and 700,000, and that the final Re would depend on

the airfoil itself. Boundary layer tripping devices seemed feasible but not realistic. Not only were they in the experimental stages but the added weight associated with such a plan would hinder the success of the mission. Serious weight discussions would be necessary to even consider adding this device. Research was performed on the testing of a single airfoil and great consequences would occur if the entire aircraft was taken into consideration. Given the technology that is available here and now, it was concluded that acoustical boundary layer control would not be used (ref 5.25).

One method which may seem feasible and, more importantly, economical would be to trip the boundary layer using the airfoil's geometry itself and by a roughening of the surface. This way, no significant amount of weight is added to the aircraft and the wing loading is not compromised. The trade-off to this method, however, is that there is a limitation as to where the low Re range may exist. Also, a high cambered airfoil may be desired since separation bubbles survive in this regime. An accurate contour of the airfoil surface to compliment the flow may aid in reducing their effect. However, overcompensation may result in hysteresis and allow a limited degree of freedom for the angle of attack. Therefore, to permit a successful mission, any Reynolds number value between 400,000 and 700,000 seems feasible depending on the airfoil chosen.

5.1.3 Airfoil Selection

Airfoil selection was determined by investigating the remaining series which survived the initial Re analysis. Detailed investigations were conducted on an XFOIL program on the Engineering Vax computers at Cal Poly Pomona. The Liebeck airfoil

(ref 5.23) showed a strong potential for selection but revealed relatively large fluctuations of boundary layer activity for the desired Reynolds number range. Also, the maximum lift coefficient which could be attained was at a value of 1.01 at a Re of 600,000. According to detailed aerodynamic calculations, the minimum lift coefficient needed to obtain level flight at 100,000 feet was 1.2. Based upon the data revealed, the Liebeck airfoil was discarded.

The Eppler 61 , 110 and 387 airfoils were also investigated for selection (ref 5.25). However, all series discovered were researched and no computer analysis was done. This was due to the fact that no airfoil geometry data points could be found to input into XFOIL and, hence, all analyses were conducted on pure research and calculations. The lift coefficients found or calculated had values which ranged from 0.93 to 1.11, but these values were generated under optimal conditions and general assumptions. In essence, no concrete information could be obtained and since the Lissaman airfoil showed the most potential, the Eppler was discarded. Upon experimenting with the Lissaman, it appeared that this airfoil, too, would not be adequate for a successful mission. When utilizing the XFOIL program, a lift coefficient of 1.12 was generated. Although this airfoil did not meet the requirements for selection, it possessed the greatest potential.

The next step seemed to be to modify the airfoil. The Lissaman 7769 airfoil was altered to slightly increase the camber toward the front third portion. This change basically allowed the airflow to be tripped toward the beginning of the airfoil and transition to a turbulent flow. This action is similar to a boundary layer tripping device. Immediate reattachment could occur and the flow would maintain a high pressure distribution. This distribution created a significantly higher lift coefficient , possessing a value of 1.2 at an angle of attack of 4 degrees. Unfortunately XFOIL showed that any value beyond an alpha of 8 degrees had some loss of lift and at alpha

of 8 degrees showed flow separation which was unrecoverable.

As a result of this modification, the airfoil selected is the Lissaman 7769 airfoil at a Re of 500,000. Since the flow apparently is highly susceptible to separation at angles of attack greater than 8 degrees, it is recommended that the climb angle for this aircraft be no greater than 7 degrees. Also, a trade-off is necessary in which some drag must be compromised for the security of the generation of lift. It is desired and recommended to have a rather large surface roughness to the wing in order to trip the flow into a turbulent mode. In this manner, the lift will be maintained and separation bubbles will be less threatening. Drag, on the other hand, will slightly be increased from one in which no surface roughness had been added. However, that value apparently is negligible when the drag of the entire airplane is taken into consideration.

5.1.4 Aircraft Aerodynamics

The primary factor which set all maximum coefficients was the engine thrust in lbs-force. According to Teledyne Continental which designed the TSIOL 550 engines, the thrust value for one engine was 500 lb-force (see Section 5.3). Since three engines are being used to propel the aircraft, a total of 1500 lb-force will be generated. Given that thrust must exceed drag to produce acceleration, the drag must be no greater than 1500 lbs. In addition to the thrust, other set parameters were included to determine the aerodynamic coefficients. These values were initially set to those similar to the Condor. By doing so, a ball-park figure could be determined and later on during the course of the analysis, the values could change depending on the trade-offs needed. The desired wing loading was arbitraraly chosen to be a value of 7. Also, the aircraft weight was established to be 26,000 lbs (see section 4.4

were generated to determine the remaining aerodynamic parameters.

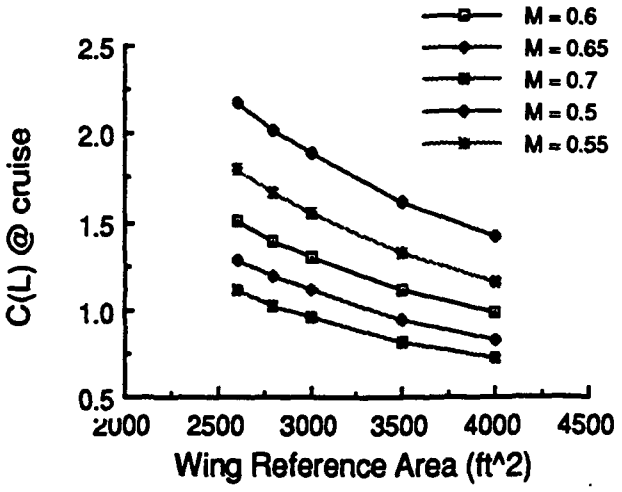

Figure 5.1: Wing Reference Area vs. Mach Number

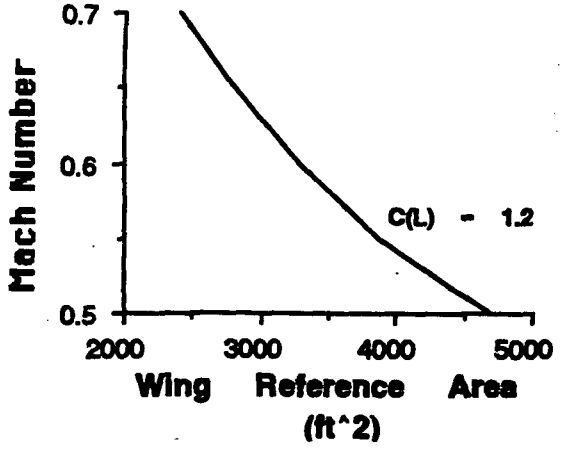

Figure 5.2: Wing Reference Area at CLmax

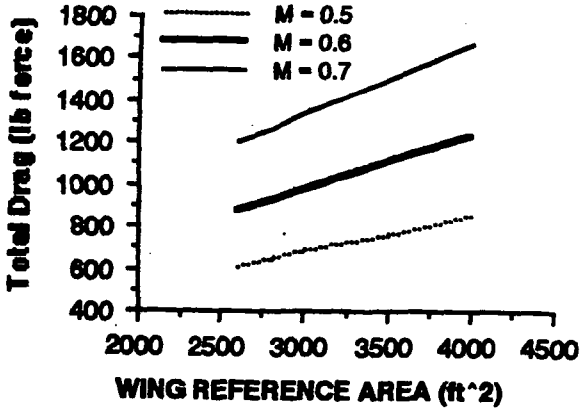

Figure 5.3: Total Drag at variable Wing Area

A parametric study on the aerodynamic characteristics was conducted and plotted to determine a range of such values. These characteristics included the surface reference area, the velocity, drag and lift coefficients, as well as wing loading and weight-to-power ratios. The majority of the plots were set with respect to the

surface reference area. In this manner, once this value was determined, other values could be immediately produced by referencing the plots.

The first graph created determined a range of surface references areas for the wing(s) (see figure 5.1). Since the RFP specified that the velocity of the plane must be in the range of 600 to 700 feet/sec (0.6 < M < 0.7), the range of values on the graph was chosen to be between 0.5 < M < 0.7. Since the lift coefficient also had a predetermined value of 1.2, the second plot was generated (see figure 5.2). This figure basically condensed the excess amount of information depicted in figure 5.1. From this chart, any Sref could be chosen and the corresponding velocity could be determined. The final plot, which completed the analysis, established the total drag of the aircraft at various speeds (see figure 5.3). This plot determined whether or not the previous parameters chosen were acceptible. If the resulting drag was less than the critical value, then it was a canidate for a set parameter. As can be seen, the total drag of the aircraft at a Mach number equal to 0.7 exceeds the thrust value of 1200 lbs-force. Hence, at speed above M = 0.7, critical drag is exceeded. Therefore, M = 0.7 could not be considers as a possible value. At a speed of Mach 0.5, however, the extrapolated values appear to be quite acceptible. But upon closer look the stall speed for the XR-1 is at a Mach number of 0.545 and thus the parameters can not even be considered for such a speed. Thorugh such detailed analysisand process of elimination, the optimal aerodynamic characterisics were determined and a ball-park figure for each value was established. From the values extrapolated, calculations revealed the optimal aerodynamic characteristics as:

Mach # = 0.6	AR= 18.9 ft^2
Sref = 3266 ft^2	Drag =1022 lbs

C(L) = 1.2	L/D= 22.5
L/D(max) = 32.2	W/S = 7.04

This analysis was performed without consideration for the structures assembly, power availabilty, and aircraft stability in mind. Hence, trade-offs were considered after these parameters were established.

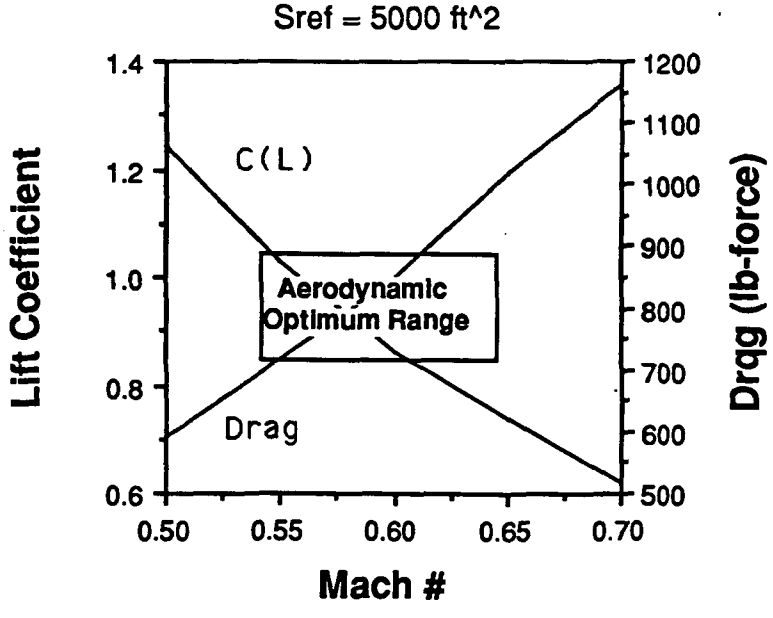

Figure 5.4: Lift Coefficient & Drag Vs. Mach Number

Due to the fact that the Mach number could not be increased beyond a value of 0.7, the XR-1 experienced problems in its propulsions and weight areas. The power generated from the three engines was not enough to achieve the desired altitude of 100,000 feet with the given weight of the aircraft. Therefore the weight had to be reduced and the surface reference area had to increase. From the performance specifications (see section 3.2) as well as maintaining the L/D as high as possible,

the surface reference area was increased from 3266 to 5000 feet^2 and the weight reduced to 26,000 lbs (see section 4.4).

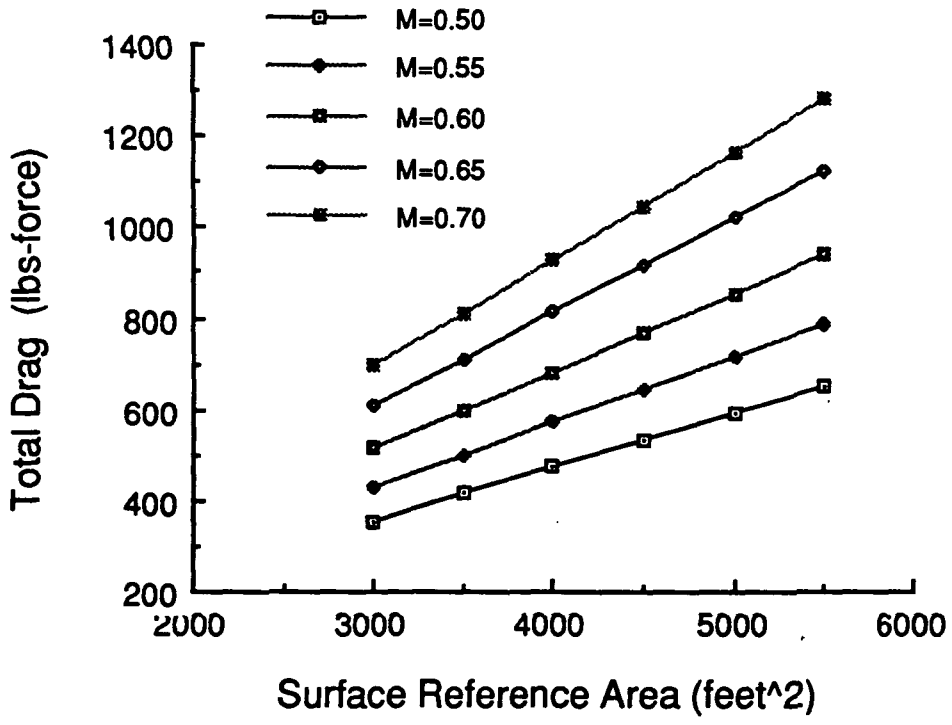

Figure 5.5: Wing Reference Area vs. Total Drag

In order to keep the drag and the wing bending moments low, the configuration was changed from a single wing to a tandem wing. As a result the AR for each wing was increased to a net value of 20. The forward wing individually possessed an AR of 16 and the rear wing possessed a value of 20. According to ref 5.33, a front wing which also poses as a canard will have 1.25 times that of the equivalent AR. Hence, the forward wing now has an AR of 20. Also an important trade-off was established with the propulsions area in which the Mach number was increased from 0.6 to 0.65. Since engine performance increased with the speed of the aircraft and the optimal range was approximately Mach =0.7, a compromise was established. From an

aerodynamics perspective, the drag has increased significantly (see figures 5.4, 5.5). However, since the aircraft configuration now has the similarity of a bi-plane, the calculated drag is reduced by 15% (see Ref 5.33).

A parametric study was again conducted using the new parameters. Since the lift coefficient had not changed, the analysis was performed for a C(L) of 1.2. (see figure 5.2). Given that the Mach number was now established at 0.65, the Sref extrapolated was 5000 feet^2. From figure 5.5, the drag was determined to be 1018 lbs. Note that this value allows all aircraft geometries to remain as desired. As a result of the tandem wing and the rather large Sref, the final aerodynamic values are as follows:

L/D = 30.1

Drag = 1018.5 lbs

W/S = 5.2

To obtain the aerodynamic coefficients for the XR-1, the drag and lift parameters were calculated at an altitude of 100,000 feet. The Reynolds number determined the parasitic drag whereas the lift coefficient determined the induced drag. Oswald's efficiency factor was determined by Ref 9. Since the wings are both highly elevated but set in an dihedral and anhedral manner, the e was chosen to be 0.65. The induced drag was computed through ref 5.27, and determined to be 0.0301. The parasitic drag was determined through ref 4. Two separate method were used to choose this value. Both were written by the same author. The two values were calculated and averaged revealing a Cd(i) of 0.0025. The reason this is such a low value is due to the fact that the surface reference area is acceptibly large and that the Re is very extremely low for standard conditions. Skin friction drag,

which was calculated from ref 5.4: section 2.1, was determined to be 0.0049. Engine cooling drag, calculated from ref 5.33, was computed at 89 lb-force. All coefficients do take into account the reduction of drag due to the tandem wing configuration. A summary of all parameters are shown in below.

Mach # = 0.65	AR	= 20 ft^2
Sref = 5000 ft^2	Drag	= 1018 lbs
C(L) = 1.2	W/S	= 5.2 lbs/ft^2
L/D(max) = 30.1 (including drag cooling factors)		

5.2 Structures and Materials

This analysis is based upon the need to create a suitable structure for the XR-1 while following the size and weight requirements established previously. Several problems must first be discussed before continuing with the analysis. First is the size of the actual aircraft. Next is the actual weight for the XR-1. Once these are established, the process of creating the structure may begin.

The design of the XR-1 is divided into several parts. These include to Wing, Fuselage, and Empennage. All three parts are designed independently, but they all will be merged to one concise design.

From the configuration portion of this report, the size and shape of the aircraft is established. The first portion to be analyzed is the wing. In order to establish a wing structure, certain information is needed. This information is the airfoil type, wing span, root and tip chords, taper ratio and any specific parameters such as twist, anhedral or dihedral angles and camber.

In order to design a structure, the inside of the wing becomes the region to work from. Since this aircraft has two large wingspans of 186 ft and 233 ft, the type of spar becomes important.

The most suitable design considered was the I-beam with several modifications. The modifications were to make use of forward and trailing edges that help to contour the shape of the wing. The edges also help in controlling moments and in essence act as a quartet I-beam design. The final design for the inside spars is the use of a multiple spar. The first two spars are located at 31% and 41% of the mean chord. This location is chosen because it is the point maximum thickness of the airfoil. The design also allows the two I-beams to act like a single torque box. This will allow all loads to be concentrated on the box for added strength. The I-beams also provide a large centralized volume for needed fuel storage. The third spar is located at 75% of the chord. This spar is used primarily for lifting devices and for control of bending moments. Finally, two smaller spars are used at the leading and trailing edges. The two spars will help to form and define the leading edge and conform to the trailing edge.

As for the ribs, a Lissaman airfoil was decided upon. This airfoil had a thickness to chord ratio of 0.12. This ratio translates well because it decreases weight. A thicker wing will increase both bending and torsional stiffness. Also a thicker wing will provide a greater wing volume which is optimal for fuel storage. With this information and the coordinates of the airfoil, the surface area of the rib is calculated. This process allows a relationship to be developed for area, thickness, and chord length. The area to chord length ratio is 0.4417 in. With this information, the actual dimensions for the I-beam may be found. Using the root chord length of the forward wing with the thickness ratio, The height of the beam is 24.58 in. Using data from other I-beams, a scaling factor for the width of the beam is developed. By

averaging the ratio of width to height for several beams, a factor of 0.454in/in is developed. With this the width of the root chord is found to be 11.16 in. Since both wings have a straight taper, the tip chord is less than the root chord. This benefits the weight aspect because taper ratios close to 1 tend to not be effective at the tip due to the fact that lift distribution at the tip leads to zero. Also fuel volume is larger at the root for a taper ratio less than 1. Therefore the I-beam must be sized to fit the wing. Using the same ratios for sizing, the beam height is 11.04 in and a width is 5.01 in. For the rear wing, the root chord height is 23.01 in and width is 10.46 in. The tip chord height is 10.37 in and a width of 4.73 in.This modeling allow for a beam to decrease in cross sectional area as the cross section moves from root to tip.

In order to simplify the calculation, a uniform beam will be analyzed. This beam will have the average dimensions for the entire wing. For the forward wing, the height is 17.81 in and the width is 8.085 in. For the rear wing, the height is 16.69 in and the width is 7.60 in. Each beam will be of uniform dimensions for this analysis.

The next aspect of the analysis is the thickness of the beam. for a preliminary concept, the unit thickness will assumed to be one inch. The I-beam cross sectional area for the average beam is 31.98 in^2 for the forward wing and 29.89 in^2 for the rear wing. An added design criteria to decrease weight is to cut holes in the ribs. Since each spar does not require the entire area to establish the shape, holes are placed within the rib. Another benefit to this is the ease for the cooling mechanisms to be placed within the wing. The cooling requirements declare that heat be dissipated throughout the wing. Therefore the holes allow for the physical mechanisms to exist within the wing.

The next portion involves the calculation of the volume and the mass for the beams. Since the average beams are uniform over the span of each wing, the volume is simply the cross sectional area multiplied by the span of the wing. For the forward

wing the volume is 7,1290.0 in^3 and for the rear wing the volume is 8,3544.5 in^3. For calculation of the weight of the beam, the material density is required. The material need to be strong yet light. Steel, Aluminum and Titanium are very excellent materials. But steel is very heavy and would not be appropriate for this type of vehicle. Aluminum is much lighter and does provide flexibility but for the size and weight of the aircraft, it is not acceptable. The same analysis applies to Titanium. A composite is now desired to fulfill the mission. Upon analysis, Graphite/Epoxy is desired. The graphite is formed in a honeycomb with the epoxy used to provide strength. The Graphite model HFT-G is being used with a quarter inch cell size.

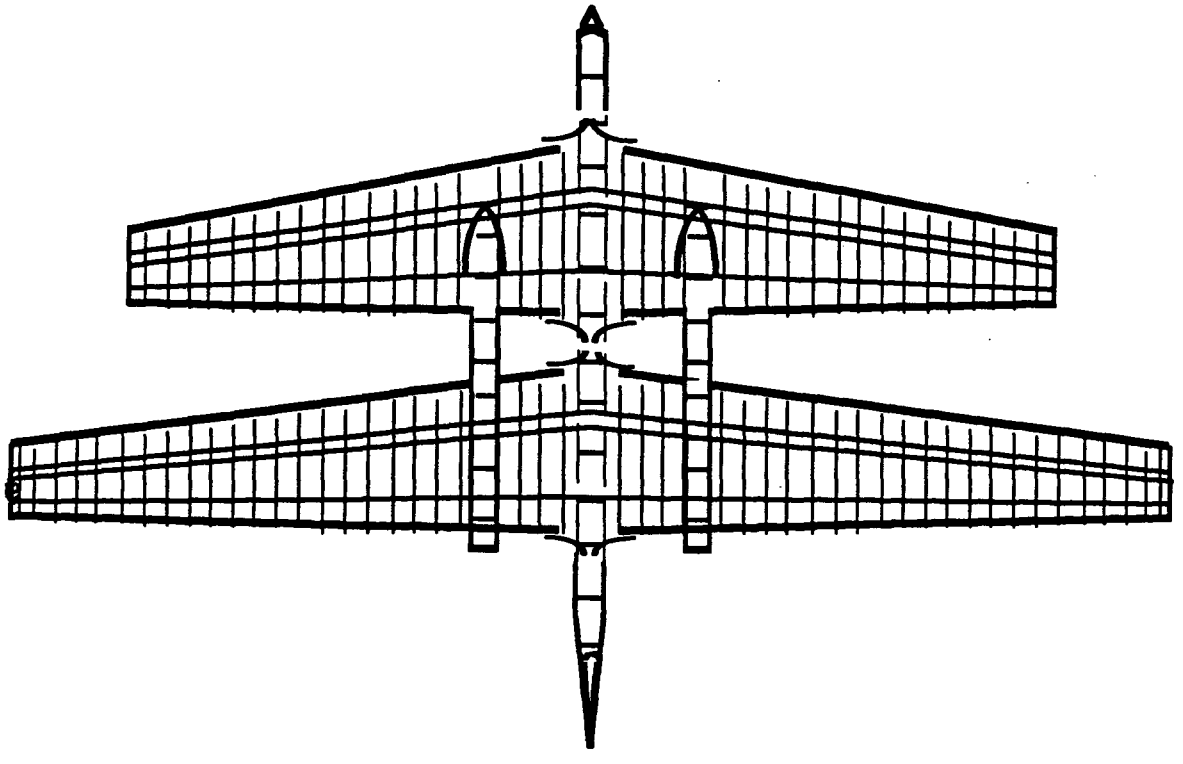

Figure 5.6: XR-1 Structural Planform

Now the internal loads must be discussed. The loads along the spars may be

calculated by several different means. The most common method is the vortex lifting line theory. Other methods include elliptical, planform or Shrenk's method. For the vortex lifting line theory, a computer program can be used to simulate the lifting loads. Since the span is symmetrical about the x-axis, only a half span is used to calculate the lift. As for choosing points for the vortices, several aspects must be looked at. Vortices may be chosen at equal intervals along the span. This is excellent for studying the effects of the loads at points located at rib positions. The only disadvantage is that as the analysis approaches the wing tip, the data gather is not as effective. Typical of loading curves, the most active changes will occur at the tip. Therefore equal intervals will not provide adequate approximations. In order to accomplish this task, a coordinate transformation by using the cosine will provide more data points at the tip for equal intervals of angle. Both these methods are valid and should both be considered in analysis. Shrenk's method of combining the planform and elliptical loading is another valid method. The combination of both all methods may still be the best method. All three method averaged will allow for "bad" data to be of a lesser influence. Now the load may be calculated and used to test the spar.

In order to shape the wing, ribs are used to accomplish this. For light aircraft, it is recommended to space the ribs at an interval of 60 inches. At this interval, the forward wing will contain 38 ribs while the rear wing will use 48 ribs. The average cross sectional area for the forward wing is 65.54 in^2 while the cross sectional area for the rear wing is 61.43 in^2. By using the number of ribs and a unit thickness of one inch, the volume of the ribs and weight can be found. This method results in a n accurate but simple way of calculating the volume and weight of the wings, and theire associated structures. The forward wing has a volume of 3932.4 in^3 and a weight of 22.768 lbs using just graphite honeycomb. For the rear wing, this results

in a volume of 4668.68 in^3 and a weight of 27.03 lbs of graphite.

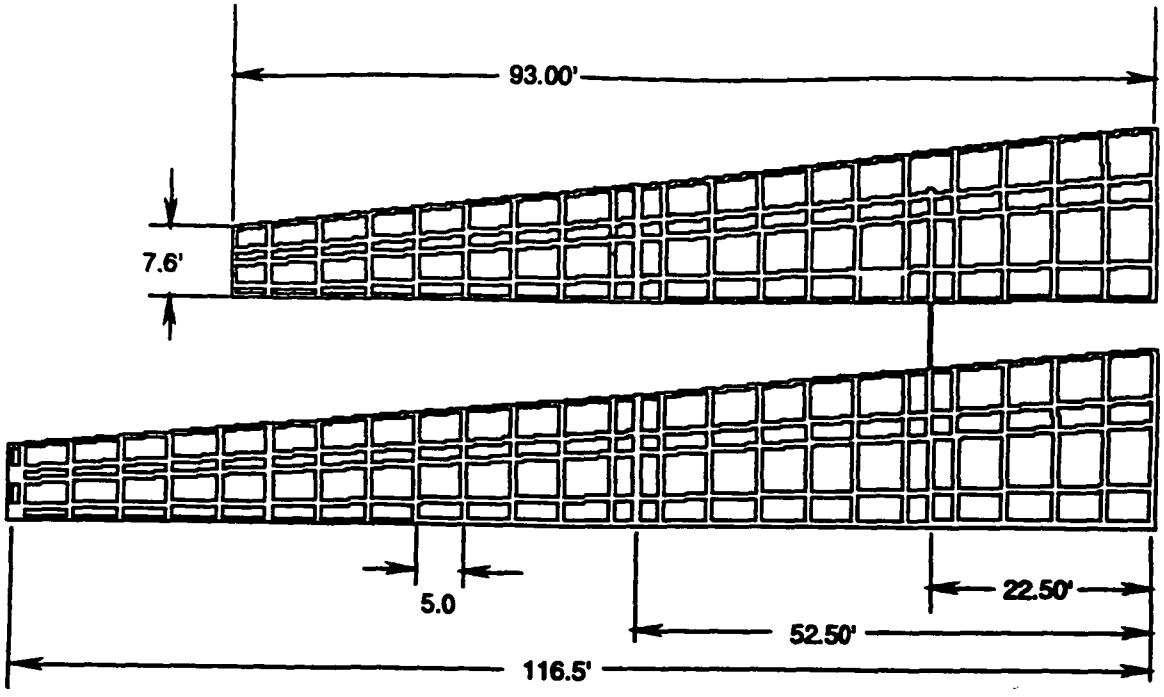

Figure 5.7: XR-1 Wing Structure

With this information, the internal loading is confirmed and the wings ability to withstand these loads is tested. Now the fuselage is to be analyzed. The length of the fuselage is 70 feet. In order to give strength to the length of the fuselage, stringers are required. A graphite epoxy will be used to provide the needed strength for the stringers. The location of each stringer is at a 45 degree interval around the entire fuselage. Ribs will also be used to hold the shape of the fuselage. The circular ribs will be at interval of 5 feet which is similar to the wing.

As the ribs approach the rear of the airplane, the ribs circular shape decreased

and the stringers converge to the rear tip. Figure 5.6 shows the internal structure of the aircraft's planforms and Figure 5.7 depicts the wing structure of the XR-1. The new concentration of the structure allows for the Vertical tail to be attached. The tail has three I-beams to provide the internal integrity while the symmetric ribs at five foot interval hold the shape to the tail. The internal beams also will provide adequate strength for controlling surfaces as shown in Figure 5.8. Figure

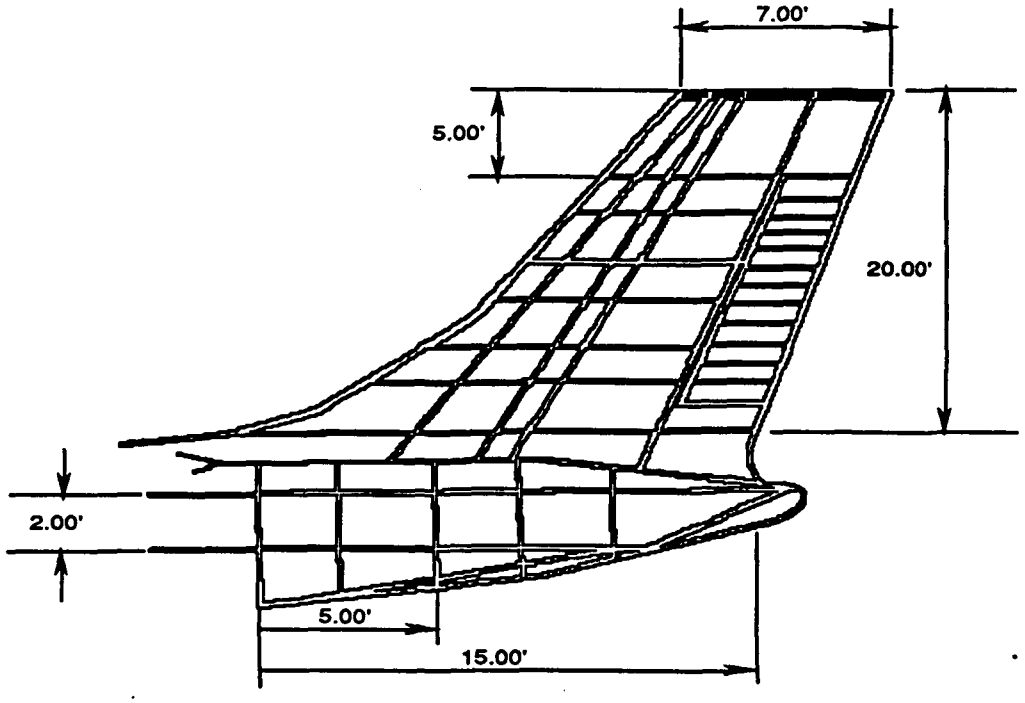

5.8: XR-1 Vertical Tail Structure

The XR-1 also has two booms. The design of the booms is also similar to the design of the fuselage with the same amount of stringers and identical distances for the ribs. The structure will help the engine weight and landing gear placement.

One detail that must be discussed is the large span of the wings. In order to allow

for the aircraft to enter the hanger, the tips of the aircraft must be removed. The removal of the tips will be at 52.5 feet from the center-line of the aircraft. This will allow a clearance of 2.5 feet on each side of the aircraft. The wings can easily be detached from the skin of the wings. The separation point is also located at a position equally between two spars. The only factor for the wing is the spar is the I-beams. The wing will use a spar that is cut at the location of the detachment. The two spar sections are attached by means of two plates of solid graphite. The plates will be attached on each side of the I-beam along the height portion of the beam. At this point, the beams are also solid graphite instead of the honeycomb and epoxy compound. To connect the plates and beams, Solid epoxy bolts will be used. Each portion of the beam will use four bolts for security. This will provide a grand total of eight bolts per half span. This design for the aircraft allows for the needed strength for takeoff and provide the necessary flexibility for cruise conditions.

5.2.1 Aircraft Operational Envelope

The operational flight strength limitations of an airplane are presented in the form of a V-n diagram. The V-n diagram for the XR-1 resulted with a positive limit maneuvering load factor of 2.767 and a negative limit maneuvering load factor of -1.00. The gust loads were determined by using Reference 5.27 Figure xx shows the V-n diagram for the XR-1 ,with the gust lines for cruise velocity, dive velocity and maximum speed in turbulence.. The airplane must be structurally able to withstand all load factors included on or within the envelope presented above

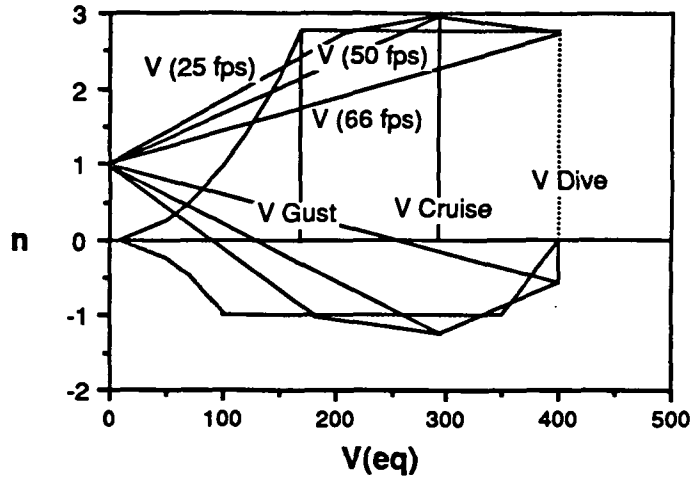

Figure 5.9: XR-1 V-n Diagram.

5.3 Aircraft Propulsion System

5.3.1 Propulsion Options

The preliminary propulsion system selection for the HAMMER was subject to several different constraints. The engine selected must have a low specific fuel consumption, due to the operational requirements of the various science missions, and it must possess a low weight as well. Both these parameters are directly related to the mission requirements.

Considerations for the selection of the appropriate propulsion system are low specific fuel consumption, low weight, and high thrust for a given size of engine. Five prime parameters can be used to determine the suitability of a given engine. These parameters are:

1. The fuel consumption in cruising flight- this is of prime importance to the range and endurance of the aircraft.

2. The specific thrust under various conditions and the decrease of thrust with altitude and speed- since the aircraft must travel at very high altitude, will the engine under consideration perform

adequately given the environmental conditions at +100,000 ft?

3. The weight and drag of the powerplant as installed the aircraft- This is important to the aerodynamic and structural design. The drag caused by the installation of the propulsion system on the aircraft is of prime importance to the designer of the propulsion system. Large engines with high frontal area will incur drag penalties that will influence the fuel consumption and thrust requirements. Higher drag means penalties that result in requirements for higher thrust with the added ramification that this increases fuel consumption and decreases the range of the aircraft. In addition, large engines will require larger and heavier structures in the aircraft, this will also affect the aforementioned parameters.

4. The noise production of the engine- this parameter is of significant important when flying over areas with high population densities

5. First cost- how much will the engine cost? For example, exotic systems which may be suitable for the mission but have to be discarded due to the high research/development and/or implementation costs

5.3.2 Turbine Engines

Obviously, mass flow rate of air is of prime importance to the production of thrust. At high altitudes (100,000+), the air density is very small, approximately 1/72 of the standard sea level values. This lack of air density makes this term very small. This means that the size of the engine must increase as the altitude increases. A turbojet sized for that altitude would have to be very large to produce adequate thrust at cruise altitude of 100,000 ft. An increase in size, is accompanied by a subsequent increase in weight. Increasing the engine weight, increases the structural requirements of the installation location placing even more constraints on the payload weight.

A turbofan is similar to the turbojet, except instead of using the excess power to eject a jet of air, the some of the power is used to drive a fan in an auxiliary duct. This fan allows air to pass around the engine,rather than through it. This auxiliary flow moves more air, but at a reduced velocity.This engine also suffers a loss in thrust at high-altitudes. In order to increase the thrust the fan diameter must be made larger. This larger diameter fan would significantly increase the drag on the engine. In addition, an engine designed to produce an adequate amount of thrust at high altitudes would be grossly oversized at sea level, and could not be used without high

5.3.3 Internal Combustion Engine

The four cycle engine has been used in aircraft since the beginning of manned flight. It is relatively simple when compared to the construction and operation of the gas turbine.

Normally aspirated engines do not have the necessary performance at the altitudes that the HAARP will be flying at. The engines need to an augmented by some sort of precompressor, to increase the air mass flow rate into the engine. Without this type of help most internal combustion engines produce no power at altitude of 15 kilometers or so. There are two ways to accomplish this task by using a turbocharger or by using a supercharger. The turbocharger uses the exhaust gases (which contain approximately 1/3 of the energy released from the fuel) from the combustion products to spin a centrifugal turbine which is coupled to centrifugal compressor placed in the air intake duct. This turbine compresses the air entering the engine, this increase in air mass flow increases the power in each cycle of the engine. Since the exhaust turbine restricts the exhaust air,it causes less efficiency burning due to the increase in back pressure. This is the most efficient way of increasing the power output of the engine. This turbocharging does not have to take place in a single stage. It is possible to break the turbocharging into several stages. The HAMMER requires at least a pressure ratio of 108 to 1 at 100,000 ft. This can be accomplished by the following engine turbocharging system:

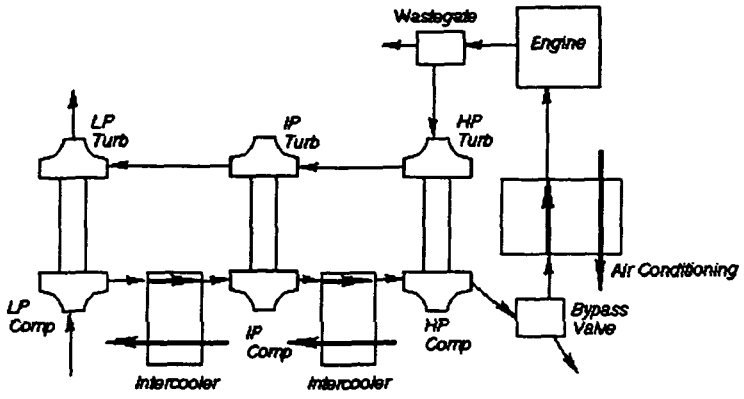

Figure 5.10: Turbocharging Schematic

The supercharger uses direct gearing to power a compressor. This compressor increases the mass flow of air and thus increases the power. However, since it is directly coupled to the engine, it does cause some power loss (6 to 10%), and also slightly increases the fuel consumption of the engine. In addition, super/turbocharging heats up the air which reduces the mass flow of air. This can be compensated for by using an intercooler, which is basically a heat exchanger, to cool the air before it enters the cylinder bank.

5.3.4 Solar Power

One possible solution to the problem of fuel weight is to use the power of the sun to power the aircraft. A typical configuration for the aircraft is to use an array of solar cells mounted to the aircraft, most likely on the wing, and upper surfaces of the fuselage to power electric motors turning propellers.

The use of solar cells as a power supply also has several implications. These group around handling, and the actual inflight flying environment. Solar cells are very

susceptible to damage, incorrect handling of the aircraft while it is on the ground can have serious consequences in terms of damage to the solar cells. Also , the use of solar power is discouraged by factors such as higher cost, weight penalties due to energy storage requirements and the need to operate during daylight hours. On the other hand, solar power has the following advantages:

The main advantages of using this type of energy source to power the motors on the HAMMER are:

1. Of the direct conversion methods, it has the highest overall conversion efficiency of solar radiation to electricity,
2. Unlimited life
3. Simplicity and ease of fabrication. Solar cells require on other equipment to operate, or in the case of the combustion engine, high temperature to obtain high efficiencies.
4. Since power is produced on board the aircraft, the fuel requirement for the mission is reduced.

5.4 XR-1 Engine Selection

The engine type selected for the XR-1 is an internal combustion recipocating engine. Out of the all the engine possibilities the internal combustion engine provides the best balance to the accomplish the mission requirements. The IC, in general, has a higher power to weight ratio than the other engine types that were studied, this coupled with the low specific fuel consumption of the IC make it the obvious choice to be the powerplant for the XR-1. The cost effectiveness and reliability of the IC were also factors in the decision to use an internal combustion engine.

The specific engine selected for the XR-1 HAMMER aircraft was a modified version of the Teledyne Continental Motor's (TCM) TSIOL-550 internal combustion

engine implementing three stages of turbocharging. The three stages of turbocharging provide a 108:1 combustor pressure ratio, thus providing enough air at 100,000 ft, where the density ratio is 72:1, to provide 500 hp of power. For the XR-1, a mission maximum of 1350 hp is required at the end of the climb phase. Thus, three of the TSIOL-550s are required providing 1500 hp at altitude. At an output of 500 hp each, a specific fuel consumption (SFC) of 0.45 lb/hp-hr results. The SFC reduces to as low as 0.39 lb/hp-hr when the engines run at 75% (1125 hp). The propulsion system; engines, turbochargers, cooling system, and accessories weigh 1900 lb each. The weights are distributed as shown in Table 5.1. The engines will be modified slightly by making use of ceramics and composites where available. This "light" engine provides a high power output for a relatively low weight. The engine is shown in Figure 5.11 below. TCM will be contracted to develop this engine with the use of ceramics and composites wherever applicable. This propulsion system accounts for 22% of the aircraft's gross takeoff weight.

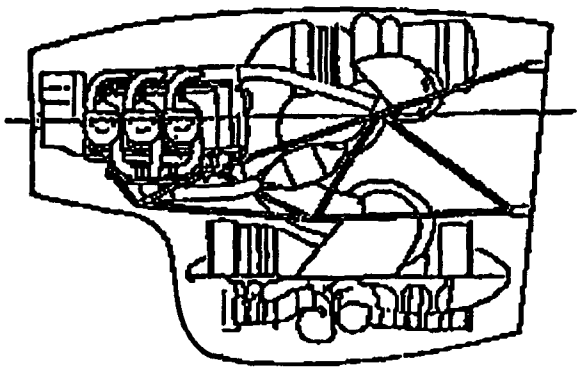

Courtesy of Teledyne Continental Motors

Figure 5.11: TCM TSIOL 550 Schematic

Propulsion System		Weight (lb)
Engine Group:	(1518 lb)	
Engine (3)		1095
Ignition (3)		81
Plugs (3 sets)		9
Exhaust Manifold (3)		36
Starter (3)		57
Gearbox (3)		150
Oil Reserves (3)		90
Turbochargers:		
HP Turbo (3)		76.5
IP Turbo (3)	(2044.5 lb)	153
LP Turbo (3)		1206
Turbo Ducting (3)		204
HP Aftercooler (3)		45
IP Aftercooler (3)		135
LP Aftercooler (3)		60
Accessory Turbine (3)		165
Cooling System		
Oil Cooler Heat Exchanger (3)		108
Radiator (3)	(1351.5 lb)	252
Coolant & Oil Lines (3)		24
Intercooler Heat Exchangers (9)		922.5
Generator/Gearbox Heat Ex. (3)		45
AV Gas Fuel System		139.5
Propulsion System Installation (10% of propusion system weight)		370.5
Cooling System Installation (20% of cooling system weight)		270
TOTAL SYSTEM WEIGHT		**5694**

Engine data for 3 Teledyne (TCM) TSIOL 550 with 3 stage turbocharging (108:1)

5.4.1 Engine Cooling

Since a piston engine is the method of propulsion for the XR-1, the removal of excess heat created by the combustion chamber must be extracted.. Since a lack of air density exists at the desired altitude, adequate heat convection cannot take place. Hence, the liquid cooling method is much more durable and provides a more uniform cooling flow thru the combustion chamber.

Other alternatives which were considered included the use of a flapped conventional radiator in combination with an internal cooling mechanism or fluid. This method only seemed to complicate the situation and was later abandoned. Weight considerations prohibited this method from its use since the aircraft was deemed to be too heavy. The flight duration would most likely then be curtailed as well as the requirement of attaining the desired altitude.

It was found that for a six cylinder reciprocating engine, the amounts of heat generated would be 15,000 and 40,000 BTU/min respective to the sources mentioned above. A study of alternatives for the engine cooling yield the following results (per engine) as shown in Table 5

Table 5.2: Engine Cooling Possibilities:

Agent	Devices	Effective Area Required	Heat Extracted
Air	Fins attached to engine block exposed to ducted air jet	50 fins @ 0.54 ft^2 ea.	8,000 BTU/min
Oil	Cavities running through engine as part of tubing loop	194 ft^2	47,000 BTU/min
Ethylene Glycol		34 ft^2	

Heat is then carried by the cooling agent (Ethylene Glycol) to aircraft surfaces for cooling by free convection. These surfaces must provide an effective cooling area of 159 ft per engine. The summary above clearly indicates that Ethylene Glycol should be used in the forced convection of the engine, as opposed to clean engine oil, because of the smaller contact area inside of the engine block that it requires.

For the mission requiring an excursion to an altitude of 120,000 ft, the use of compressed liquid Nitrogen at 100 K, loaded at sea level is recommended. This additional mechanism would be able to remove an additional 15,000 BTU/min of heat expected in the climb. The superheated Nitrogen would be bled out of the tubing system via the wing tips. In the development of this study the following assumptions were made: the engine block remains at a constant mean temperature of 560 K,in the process of free convection by air on the fins the flow does not reach turbulence, all processes of heat exchange are 100% efficient, and the flow remains laminar throughout the engine inlets.

Consequences involved in the engine cooling process include drag penalties as well as structural weight considerations. The cooling drag associated with this process was determined to be a value of 82 lbs-force. This is a significant factor in the total drag calculated but, due to the aircraft configuration, this penalty does not pose a serious threat. Added tubing and pumps within the wings and fuselage must be incorporated to ensure proper cooling.

5.5 Power Requirement Determination

The aircraft's power requirement was determined by looking at a trade-off between wing surface area, weight, and technology available. In order to keep the

cost of the propulsion system at a minimum, the design of a complete new engine is not warranted. Upscaling a current model however, is within the budget for the HAMMER aircraft. The reference area will be split between two wings on the XR-1 design. A maximum wing area of 5000 lb will be chosen to limit the weight and structural concerns of the tandem wing surfaces. The climb speed will not be permitted to increase above 650 fps in order to avoid tip shocks on the propeller and rest of the aircraft. At weights above 27,000 lb, speeds in excess of this speed are inherent, and must therefore be left out. This gives the clearcut region of requirements to choose from.

The wing area was maximized to provide a maximum amount of lift at cruise, thus allowing the weight to minimize. Based on the maximum allowable power (1500 hp) and the reference area of 5000 ft, a gross takeoff weight of 26,000 lb was found to be substantial. The actual weight of the aircraft upon reaching the cruise altitude will be less (~24500 lb), thus allowing the engines to be run below full throttle once 100,000 ft is reached.

5.6 Propeller Design

Basically a propeller blade may be modelled as an aircraft wing, however, the lift produced will be acting parallel to the velocity vector of the aircraft, not perpendicular to it as the lift produced by a wing would. For a wing, a large value for the lift coefficient is desired to maximize the amount of lift for the aircraft. For a propeller blade, the main design drivers do not necessarily include the lift coefficient. It was decided that the propeller diameter, the efficiency of the propeller, the advance ratio and the tip speed were the most important criteria for the propeller design. The diameter of the propeller was limited by structural and weight constraints, excessive

tip speeds for large diameter propellers, and ground clearance considerations. Yet, the larger the propeller, the greater the amount of thrust may be produced. This becomes increasingly important at higher altitudes where the air is less plentiful. After taking all of these factors into consideration, a maximum diameter for the propeller was set at 25 feet. Beyond that, the tip speeds exceed Mach 1 at which point the propeller efficeincy is highly degraded.

Propfan technology has been around for several years and is currently being used on aircraft. Since it is current technology, it is possible that an off-the-shelf model may be acquired. If not, a certain propfan design may only need minor modifications for the requirements of the aircraft, such as a larger diameter. A view of a typical advanced propfan propeller is shown in Figure 5.12. Some of the current statistics of the propeller are as follows. Propfans usually have eight or ten blades and have diameters ranging anywhere from 2 to 20 feet. The chosen diameter for the HAMMER propfans is 20 feet. This gives sufficient ground clearance and does not pose any structural difficulties.

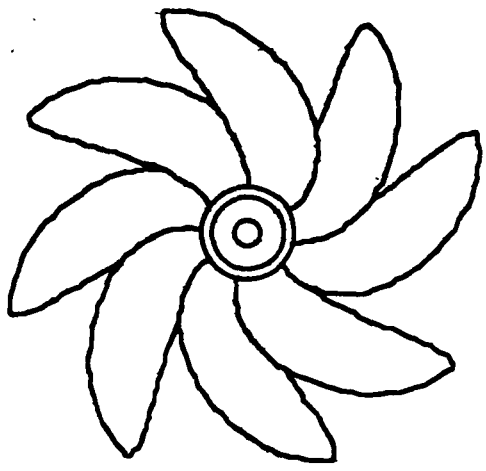

Figure 5.12: Advanced Propfan Propeller

The design efficiency of the propfan is approximately 0.90. This high efficiency is not only possible at higher (subsonic) Mach numbers, but the propeller was actually designed for a Mach range of 0.6 to 0.8 without significant loss of propeller efficiency. Other advantages for the propfan include a smaller diameter than an ordinary propeller due to the high curvature of the blades and the high efficiency of the propfan, larger solidity factors due to the increased blade area (which helps increase the efficiency of the propeller), and a greater fuel efficiency (13-25% savings) than from a conventional propeller due to the increased efficiencies. In addition, greater tip speeds may be maintained due to the high degree of sweepback of the propfan blades. In order to reduce the weight as much as possible, the blades will be construted from composite materials, mainly graphite-epoxy with an outer coating consisting of a nickel shell. Sandwich construction is not really needed in this instance since advanced airfoil sections are used for the propeller blades, and the result is a much thinner blade than would be found on a conventional propeller which would most likely use a NACA six-series airfoil. The most readily availible information concerning the advanced propfans may be obtained either from NASA or from Hamilton Standard.

5.7 Aircraft Stability and Control

The aircraft stability and control was analyzed using several different methods. These methods include both classical controls theory and modern or state space theory. The stability is designed from the cruise condition since this is where the aircraft would spend most of its time. The extreme variation in density between sea level and 100,000+ft complicates the analysis, and requires the breakdown into different flight phases. For the sake of simplicity

the stability analysis was divided into fourdifferent phases: take-off, climb and cruise. The appropriate aerodynamic coefficients and derivatives were calculated for these three different flight phases. Three assumptions were made regarding the analysis 1) the aircraft was a rigid body 2) Stability coefficients do not vary greatly while the aircraft is in cruise and 3) the aircraft mass distribution (i.e. the moments of inertia do not vary greatly as the aircraft burns fuel. The Reference 5.28 was used to determine the flying qualities of the aircraft.

5.7.1 Aircraft Stability Derivatives

The longitudinal and lateral stability derivatives were calculated by using a in-house software package known as Staderp (for Stability Derivatives). This spread-sheet program is a computerized version of Reference 5.33 The four aircraft flight phases that the control analysis was carried out for are defined in Table 5.3.

Table 5.3.1: Summary of Flight Phases

	Altitude (ft)	Speed (fps)	Weight (lb)
Phase 1: Takeoff	Sea Level	100	26,000
Phase 2: Begin Cruise	100,000	644	24,500
Phase 3: End Cruise	100,000	644	20,500
Phase 4: Landing	Sea Level	100	19,000

The derivatives for the various flight phases are shown in Table 5.4 and Table 5.5.

5.7.2 Longitudinal Static Stability

The HAMMER has an inherent static stability with a static margin of approximately 15% over the entire center of gravity travel. Since the aircraft has two wings, the forward wing is much like a canard and it adds a destablizing moment to the aircraft. However, by locating the center of gravity in the proper location it is possible to eliminate the destabilizing aspect of the aircraft. The aircraft is now basically a large fuel tank. The fuel was evenly distributed through out the aircraft to keep the plane statically stable.

Table 5.4.2: Summary of Longitundial Stability Derivatives

Derivative	PHASE 1	PHASE 2	PHASE 3	PHASE 4
C_{D_α}	0.098	0.201	0.166	0.072
C_{D_u}	0.000	0.000	0.000	0.000
$C_{L_{ic}}$	1.203	1.500	1.500	1.203
$C_{M_{ic}}$	-1.806	-2.249	-2.249	-1.806
C_{L_α}	5.647	7.079	7.079	5.647
C_{L_U}	0.004	0.502	0.416	0.003
C_{L_q}	13.78	17.292	17.29	13.78
$C_{L_{\delta_e}}$	0.314	0.391	0.391	0.314
$C_{L_{\dot{\alpha}}}$	-14.93	-25.250	-25.25	-14.93
C_{m_α}	-2.298	-2.988	-2.988	-2.298
C_{m_u}	0.000	0.000	0.000	0.000
C_{m_q}	-16.85	-21.148	-21.148	-16.853
$C_{m_{\delta_e}}$	-0.396	-0.492	-0.492	-0.396
$C_{m_{\dot{\alpha}}}$	0.896	1.296	1.296	0.896

*Note: All derivatives are per radian (except those involving control inputs)

5.7.3 Longitudinal Dynamic Stability

At take-off, the HAMMER possesses inherent stability, however, as the HAMMER continues to climb the stability coefficients vary quite a bit which plays havoc with the stability of the aircraft. This necessitates the use of a stability augmentation system to provide adequate flying qualities for the aircraft. The flying qualities were evaluated by using Reference 5.28. Although the primary configuration for the aircraft is unmanned, the Reference 5.28 was still used as a guide to evaluate the aircraft an show any deviances.

Table 5.5: Lateral Stability Derivatives

Derivative	PHASE 1	PHASE 2	PHASE 3	PHASE 4
C_{y_β}	-0.3145	-0.3227	-0.3227	-0.3145
C_{y_p}	-0.0132	-0.0121	-0.0132	-0.0145
C_{y_r}	0.0628	0.0651	0.0649	0.0625
$C_{y_{\delta_r}}$	0.0145	0.0149	0.0149	0.0145
C_{l_β}	0.0777	0.0775	0.0772	0.0774
C_{l_p}	-0.4008	-0.5205	-0.5205	-0.4008
C_{l_r}	0.1743	0.3036	0.2617	0.1446
$C_{l_{\delta_a}}$	0.1534	0.1993	0.1993	0.1534
$C_{l_{\delta_r}}$	0.0004	0.0003	0.0004	0.0004
C_{n_β}	0.0290	0.0302	0.0301	0.0289
C_{n_p}	-0.0370	-0.0579	-0.0479	-0.0273
C_{n_r}	-0.0160	-0.0243	-0.0202	-0.0137
$C_{n_{\delta_a}}$	-0.0050	-0.0107	-0.0089	-0.0037
$C_{n_{\delta_r}}$	-0.0017	-0.0018	-0.0018	-0.0017

*Note: All derivatives are per radian (except those involving control inputs)

5.7.4 Lateral Dynamic Stability

Using a stability augmentation system, and state space methods the lateral modes (dutch roll, spiral, and roll) were modified from their previous unstable locations to locations that corresponded with MIL 8785 Level 1 flying qualities. This was done using the lateral state space matrices and pole placement techniques to yield the required eigenvalues for the system. The pole placement action resulted in a matrix of gains: full state feedback.

Table 5.6: Uncompensated Longitudinal/Lateral Modes

	Mode	PHASE 1	PHASE 2	PHASE 3	PHASE 4
Longitudinal	Phugoid	-0.1576 1.602	0.0008± j0.10851 ω_n= 0.109 ζ=-.00074	-0.0069± j0.1173 ω_n= 0.117 ζ=-0.0589	-0.1748± j0.5 ω_n= 0.529 ζ= 0.3292
	Short Period	-47.95± j5.94 ω_n= 48.3 ζ= 0.99	-0.4668± j2.653 ω_n= 2.69 ζ= 0.1733	-0.5196± j2.6557 ω_n= 2.7 ζ= 0.192	-4.6 -42.15
Lateral	Roll	-40.83	-1.0142	-0.8667	9.135
	Spiral	-0.2422	-0.0466	-0.4147	0.1139
	Dutch Roll	-0.1762 0.0644	-.3533 1.7451	1.7923 0.0387	-1.208± j0.3669 ω_n= 1.26 ζ= 0.9569

*Note: All boldfaced quantities are unstable

5.7.5 Stability Augementation Systems

Longitudinal Stability Augmentation Systems:

Since the stability of the aircraft is clearly in need of help stability augmentation systems were employed to improve the response and stabilize the various modes of the aircraft motion. In the longitudinal directions, the unstable phugoid was stabilized by using rate feedback in the implementation of a pitch displacement autopilot. By the correct selection of the gain for the rate gyro in the inner feedback path, the unstable phugoid was stabilized.

Lateral Stability Augmentation Systems:

As evident from Table 5.6, the lateral modes for almost all the flight phases were unstable. For a majority of the flight phases, the spiral and dutch roll modes are unstable. Rather than using the trial and error classical methods of augmenting the lateral stability of the aircraft, it was decided to use modern state space techniques. The procedure involved using full state feedback to accomplish pole placement. This was done by using MIL 8785 as a guide for level one flying qualities.

5.7.6 Autopilots

Automated Landing System

The main lateral autopilot is associated with the automated landing system. The automatic lateral beam guidance system. the system has a localizer beam located along the centerline of the runway, control system aboard the aircraft senses this beam and aligns the aircraft up with it. The autopilot has the intercept angle, lambda, as the input and outputs a suitable correction.

Pitch Displacement Autopilot

The primary longitudinal autopilot the was designed was a simple pitch displacement autopilot with rate feedback to damp the phugoid motion of the aircraft. As can be seen in the time response for a 1 degree elevator step, the system has adequate damping and a reasonable level of overshoot (10%). A lag was placed into the forward loop to correct the 10% steady state error the system exhibited, this lag approximates an integrator which changes the type of the system (from type 0 to type 1). The Forward and Loop Gains were chosen on a trial and error basis and selected to be Kamp=20, Krate gyro=1.8.

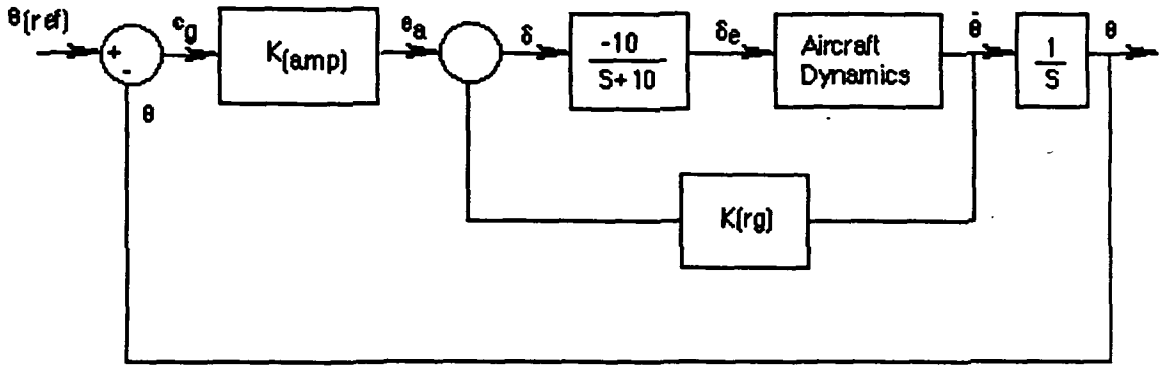

Figure 5.13: Pitch Displacemnt Auto Pilot

Mach hold/Altitude hold Autopilot

These two autopilots are integral to the design of the overall control system. Since the aircraft must remain at steady altitude the altitude hold autopilot is a necessity to avoid having the aircraft be under direct pilot control at all times.

The autopilot uses elevators, and engine throttles controls to keep one or the other constant. The block diagrams of the systems designed for this aircraft are shown in Figure 5.14.

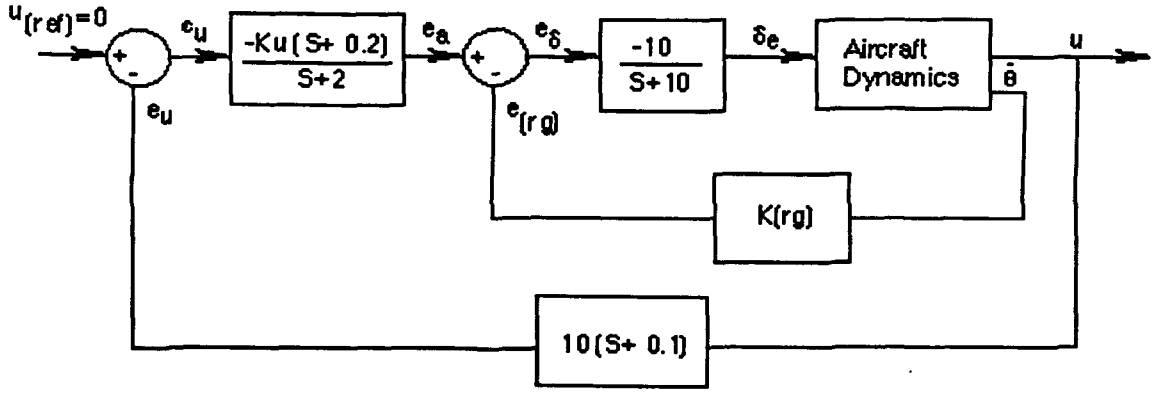

Figure 5.14 Mach Hold Autopilot

Gust Load Alleviation System

Due to the very low wing loading exhibited by the HAMMER the aircraft will be highly suspectiable to gust and wind loads. It will be necessary to implement a gust load alleviation system on the aircraft to reduce the structural loads placed on the aircraft by atmospheric turbulence. By using this system it will be possible to keep the low wing loading on the aircraft without increasing the structural weight of the aircraft. Now it would be able to withstand the atmospheric turbulence.

The primary flight control will be accomplished using a integrated flight control system (IFCS). All flight controls and other scientific sensing will be accomplished remotely using this system. The implementation of this system is demostrated in the

block diagram Figure 5.15. All the aircraft systems and subsystems will be tied int the IFCS. The computer will interface with a scientific control computer(SCC) which will control all the scientific equipment and collect the data returned from the sensors for storage in the flight recorder. This information will also be relayed directly to the NASA test facility (NFT). The telecommunications will consist of three recievers: 1)Global Positioning Satellites (GPS) system for accurate position,velocity and acceleration measurement 2)Shortwave Receiver to recieve commands from the NTF, and 3)Navigational Radios (ILS-instrument landing system, OMNI reciever, LORAN C/D) to provide navigation aid, especially during takeoff and landing. These three recievers will be directly tied to the flight management computer. The one transmitter aboard the aircraft will relay both navigational data (i.e. GPS position,speed, altitude etc) and the acquired data back to the NTF.

The flight control aspects of the IFCS are as follows: the inputs consist of flight velocity,vertical velocity, pitch angle, sideslip angle, roll rate,roll angle, yaw rate and yaw angle. These are sensed by the appropriate rate gyros mounted in the fuselage. The autopilot controls laws are located in the flight control module. The outputs from the flight computer are elevator, rudder, aileron and throttle control signals. While in flight the flight control module compares the preprogrammed flight plan with the navigational data provided by the GPS system and the navigational radios and any difference is corrected by the appropriate control signal. Any flight changes mandated by the NTF will also be processed with the IFCS,and implemented using the required control signals to the proper control surfaces (or throttle).

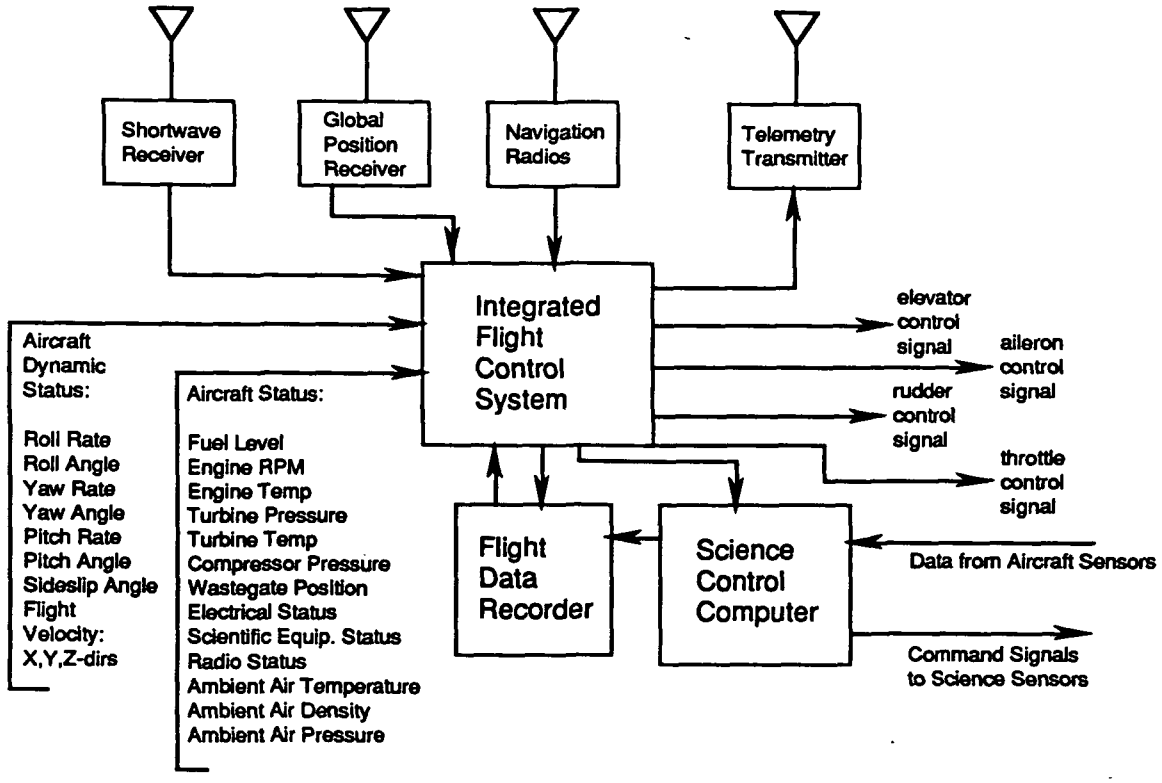

Figure 5.15: Intergrated Fliight Control System

5.8 Landing Gear

Three types of landing gear were considered. The first one, was a detachable type of landing gear, second type, the tricycle arrangement, and finally, the bicycle type arrangement with outriggers in the booms to help support the weight of the two engines, and wings was considered.

For landing, the aircraft would use the two support landing gears located on the booms, and then rest the airplane on a dollie type of landing gear,awaiting on the

runway. This type of landing gear it would save about 400 lb of the takeoff gross weight, but the following problems would be encountered with this type of landing gear :

•The landing gear would have to be in several landing locations.

•If the aircraft needed to make an emergency landing somewhere else the landing gear would not be there.

•Difficulty to catch the dollie at landing since it is remote controled.

•The landing gear on the booms must be extremely long.

The bicycle landing gear arrangement has two main wheels on the fuselage. One fore and one aft of the c.g., with small outrigger wheels on the booms to help with the distribution of weight and at the same time to help the aircraft from tipping sideways. This type of arrangement has the aft landing gear behind the c.g. in such a location that the aircraft must takeoff and land in a flat attitude, but for our particular aircraft the large surface area creates great amounts of lift and thus presents no problems in that respect.

Having analyzed these three previous arrangements of landing gears, the bicycle type of arrangement was selected. Having determined the most forward and most aft locations of the c.g.. The nose landing gear was placed 16 feet from the back of the front propeller, and the main landing gear was placed 50 feet from the back of the front propeller. The landing gear loads were calculated for the front and main landing gear. These loads are showed on below:

Max. Static Load ..... 13,765 Lbs.

Max. Static Load (nose) ..... 13,765 Lbs.

Min. Static Load (nose) ..... 12,235 Lbs.

Dynamic Braking Load (nose) ..... 3,090 Lbs.

load per tire ..... 6,883 Lbs.

The diameter and width are the same for the main and nose landing gear, being 32 inches and 9.8 inches, respectively

Once the values for diameter and width were determined, 9.50–16 Type III tires were selected. A Type III tire, such as 9.50–16, refers to the approximate tire width (9.2–9.8 in.) and wheel rim diameter of 16 in. The Type III was selected over the Type VII because the Type III is used for most piston aircraft and the Type III has a wide tread and low internal pressure. On the other hand the Type VII tires are used mostly on jet aircraft, and are designed for higher landing speeds. The footprint area was found to be 81.5 square inches. Once the footprint area was calculated, the inflation pressure was calculated to be 85 psi. The 9.50–16 Type III tire has an inflation pressure of 90 psi. therefore the tire selection is still with in range.

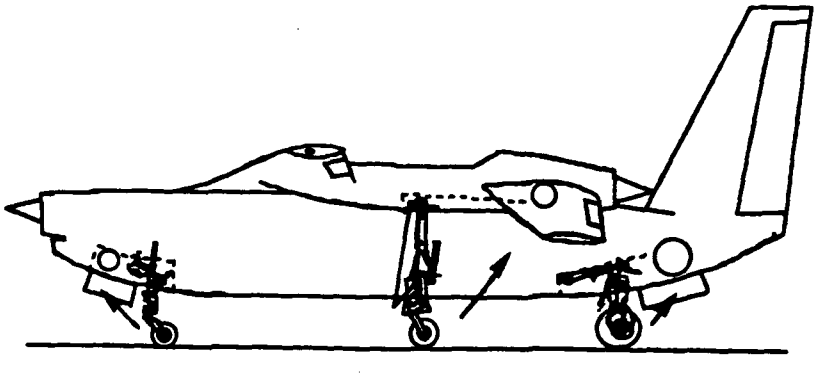

Figure 5.16: XR-1 Landing Gear Configuration

The Kinetic Energy per braked wheel was calculated to be approximately 21,800,000 ft–Lbs/sec. Using expensive, complicated brakes the wheel diameter

does not need to be increased. The oleopneumatic type of shock absorbers are to be used in the HAMMER aircraft. The stroke was calculated to be 16 inches, and since the length of the oleo is approximately 2.3 times the stroke, the oleo lengthwas calculated as 36.8 inches. The oleo diameter was calculated to be 4.7 inches. Adding the stroke, oleo, and tire with rim the total length of the landing gear resulted in approximately 7 ft, more than sufficient to clear the propeller of the ground. Figure 5.16 shows the XR-1 landing gear configuration.

The nose landing gear will retract towards the front, and the main landing gear will retract to the back.

The outrigger landing gear are mainly to keep the aircraft from tipping to one side. The outrigger is not designed to take any of the main loads that occur at landing. The outriggers will help stabilize the aircraft once it has landed. The outrigger will be stored inside the boom under the main wing.

5.9 Ground Handling

The HAMMER aircraft will have a detachable type of wing, since the aircraft would not fit in the 70 x 110 hangar that NASA has for this type of aircraft. The wing will be detached at a distance of 55.5 feet from the centerline of the aircraft. This applies to both wings and provides for a clearance of 2.5 feet on each side from the hanger walls. The remaining portions of the wing can be stored along the sides of the hanger. The wing portions will be attached and removed by use of a standard forklift that is a common vehicle to all landing facilities. Therefore the aircraft will require assembly before takeoff.

From the hangar, the XR-1 can be towed outside to an assembly station. The station requirements are that of an area sufficient to allow the wing span to stand

unobstructed. Once the airplane is towed outside of the hanger, the wings will then be attached. Only one forklift is required for this process. The forklift will bring out each section of wing and will also be used to lift and place the section to the aircraft. To carry each section, two straps will be wrapped around each section and be lifted and transported by the forklift. Once the section is in position, the section will be attached to the main body of the aircraft at the spars. The wing section will have sleeves on each side of each I-beam. The sleeves will then be slid over the main wing body and will be attached with four bolts for each spar. Once in place, the bottom wing access panel will be replace and the straps will be removed. Due to the location of the landing gear at the engine boom, the aircraft will not tip when one portion is attached. The forklift will then return to the hanger and retrieve the next section. The next section must be for the opposite side of the XR-1. This will provide the necessary balance and symmetry to prevent unnecessary loads on the aircraft. The following three sections will be attached using the same method as above.

Once assembled, the XR-1 will be fully fueled and checked for basic system integrity. Now the aircraft can be towed to the runway for take-off. At the take-off position, the full system check will be conducted. This system check will be overseen by the PETO and upon completion, the aircraft will take-off.

For ease of use, the aircraft will be towed to and from the runway. After the mission, the aircraft will be towed back to the hanger and can be disassembled in reverse order of assemble. Once disassembled, the XR-1 will be placed back into the hanger and stored safely.

5.10 Crashworthiness

Most of the safety considerations that apply to manned aircraft in the event

of a crash do not apply to our unmanned configuration. For example, the location of the fuel stores, engines, and the positioning of floor struts does not depend on the location of the crew or the pilot. Instead, other more relevant design parameters, such as location of the center of gravity, have influenced the location of the various aircraft components.

However, a firewall that is angled-in at the belly of the aircraft, between the front engine and the rest of the fuselage will be necessary to protect most of the structure from further damage upon a crash. The location of the fuel stores high in the wings and close to the fuselage provide a lesser risk of fire due to impact against objects on land. However, in the event of a belly landing or crash, the second wing is likely to sustain extensive damage at the tips because of the wing anhedral. Similarly, the front engine and its respective propeller will be considerably damaged or destroyed.

An important concern is whether the data acquisition systems, the avionics system and other electronic equipment merit the weight investment to enhance their survivability in a crash. Since the design group has no information as to the value (cost, availability, etc.) of such equipment, a decision to this effect cannot be made at this point.

5.11 Maintainability

Some of the maintenance considerations in the design of this aircraft are:

ENGINES: Mounted in the nose of the aircraft and on the wings, the cowlings should be lightweight. They should be hinged panels providing easy access to the engines to allow convenient engine maintenance.

AIRCRAFT SURFACES: The surfaces are to be washed and free of any dirt or insects before each mission, this is necessary as to not compromise with unnecessary skin drag the dynamic characteristics of the aircraft.

WINGS: The wing tips need to be detached before storing the aircraft in its respective hangar.

References

5.1 Allen, David H. and Walter E. Haisler: Introduction to Aerospace Structural Analysis. John Wiley and Sons, New York, 1985.

5.2 Allen, John E.: Aerodynamics- The Science of Air in Motion. McGraw-Hill Book Co., Inc., New York, 1982.

5.3 Arndt, William E.: "Propfans Go Full Scale", Aerospace America. pp. 100-103, January, 1984.

5.4 Bertin, John; Smith,M.: Aerodynamics For Engineers, 2nd ed. Prentice-Hall, New Jersey, 1987.

5.5 Bockris, J.: Energy: The Solar-Hydrogen Alternative. John Wiley and Sons, New York, 1975.

5.6 Campbell, Ashley S.: Thermodynamic Analysis of Combustion Engines. John Wiley and Sons, New York, 1979.

5.7 Cumins, C. Lyle: Internal Fire. Society of Automotive Engineers, Warrendale, Pennsylvania, 1989.

5.8 Drela, Mark: "Low Reynolds number Airfoil Design for the M.I.T. Daedalus Prototype: A case study", AIAA Journal, Vol 25, No. 8, pp. 724-732, August 1987.

5.9 FAA Statistical Handbook of Aviation. U.S. Department of Transportation, U.S. Government Printing Office, Washington D.C., 1988.

5.10 Fei-Bin, Hsiao, Chin-Fung Liu and Zen Tang: "Aerodynamic Performance and Flow Structure Studies of a Low Reynolds Number Airfoil" AIAA Journal, Vol. 27, No. 2, pp. 129-139, February 1989.

5.11 Green, Martin A.: Solar Cells: Operating Principles, Technology, and System Application. Prentice-Hall, Inc., New Jersey, 1982.

5.12 Green, W. L.: Aircraft Hydraulic Systems. John Wiley and Sons, New York, 1985.

5.13 Gregory, D. P.: Fuel Cells. M&B Monograph CE/7, Crane, Russak & Company, Inc., New York, 1972.

5.14 Hager, Roy D.: Advanced Turboprop Project. NASA Scientific and Technica

lInformation Division, 1988.

5.15 Hamilton Standard Division of United Technologies.

5.16 Harvey, William D.: "Low Reynolds Number Aerodynamics Research at NASA Langley Research Center", Presented at a seminar for Fluid Dynamics, St. Louis, Missouri, 1986.

5.17 Henderson, Breck W.: "Boeing Condor Raises UAV Performance Levels", Aviation Week & Space Technology. Vol 132, No. 16, April 23, 1990.

5.18 Hoblit, Frederic M.: Gust Loads on Aircraft: Concepts and Applications. American Institute of Aeronautics and Astronautics, Inc., Washington D.C., 1988.

5.19 Horener, Sighard: Fluid Dynamic Drag. Published by author, Great Britain, 1985.

5.20 Incropera, Frank P. and David P. DeWitt: Fundamentals of Heat and Mass Transfer. John Wiley and Sons, New York, 1985.

5.21 "Knowledge Based Concepts and Artificial Intelligence: Applications to Guidance and Control", Advisory Group for Aerospace Research and Development. AGARD Lecture Series No. 155, 1987.

5.22 Larrabee, Eugene E.: Propeller Theory: Design and Analysis. Illustrations for a lecture, March 1987.

5.23 Liebeck, R.H.: "Low Reynolds Number Airfoil Design at the Douglas Aircraft Company", Presented at a seminar at Douglas Aircraft Co., Long Beach, Califor nia, March 1986.

5.24 Linden, David: Handbook of Batteries and Fuel Cells. McGraw-Hill Book Com pany, New York, 1984.

5.25 Managalam, S.M. and A. Bar-Sever: "Transition and Separation Control on a Low Reynolds number Airfoil" Paper No. 10, Presented at AGARD Fluid Dynami cs Panel Symposium on Unsteady Aerodynamics, Ottawa, Canada, September 1987.

5.26 McClellan, J. Mac: "Power House: New Lines of Turboprops and Pistons from Teledyne Continental", Flying. Vol. 115, October 1988.

5.27 McCormick, Barnes W., Jr.: Aerodynamics, Aeronautics, and Flight Mechanics. John Wiley and Sons, New York, 1979.

5.28 MIL-F-8785C. Military Specification, Flying Qualities of Piloted Airplanes, 1980.

5.29 "The NAVSTAR GPS System", Advisory Group for Aerospace Research and Development. AGARD Lecture Series No. 161, 1988.

5.30 Oates, Gordon C.: Aerothermodynamics of Gas Turbine and Rocket Propulsion. American Institute of Aeronautics and Astronautics, Inc., Washington D.C.,

1988.

5.31 Pallett, E. H. J.: Automatic Flight Control. BSP Professional Books, Oxford, England, 1987.

5.32 Powell, J.: Aircraft Radio Systems. Pitman Publishing Limited, London, England, 1981.

5.33 Raymer, Daniel P.: Aircraft Design: A conceptual Approach. American Institute of Aeronautics and Astronautics, Inc., Washington D.C., 1989.

5.34 Richardson, Donald V.: Handbook of Rotating Electric Machinery. Reston Publishing Company, Inc., A Prentice-Hall Company, Reston, Virginia, 1980.

5.35 Roskam, Jan: Airplane Design. Roskam Aviation and Engineering Corp., Ottawa, Kansas, 1985.

5.36 Shepherd, Dennis G.: Aerospace Propulsion. American Elsevier Publishing Company, Inc., New York, 1972.

5.37 Shevell, Richard S.: Fundamentals of Flight. Prentice-Hall, Inc., New Jersey, 1989.

5.38 Smith, G.: Storage Batteries: Including Operation, Charging, Maintenance and Repair. Pitman Advanced Published Program, Boston, Massachusetts, 1980.

5.39 Solar Cell Array Design Handbook. Volume I, Jet Propulsion Laboratory, National Aeronautics and Space Administration, October 1976.

5.40 Sonntag, R. E. and G. Van Wilen: Introduction to Thermodynamics: Classical and Statistical. John Wiley and Sons, New York, 1982.

5.41 "Specifications: Aerospace Forecast and Inventory", Aviation Week & Space Technology. Vol 132, No. 12, March 19, 1990.

5.42 Stevenson, Greg: "Internal Fire Versus External Desire", Unmanned Systems. Winter 1990.

5.43 Stinton, Darrol: The Design of the Aeroplane. BSP Professional Books, Boston, Massachusetts, 1983.

5.44 Sutton, George W.: Direct Energy Conservation. McGraw-Hill Book Company, New York, 1966.

5.45 Teledyne Continental Motors.

5.46 Tetley, L. and D. Calcutt: Electronic Aids to Navigation. Edward Arnold, London, England, 1986.

5.47 Torenbeek, Egbert: Synthesis of Subsonic Airplane Design. Delft University

Press, Nartinus Nijhoff Publishers, The Hague, Holland, 1982.

5.48 Valey, Helen: The Air Traveller's Handbook. Simon & Schuster, New York, 1980.

5.49 Ward, J.W.: "The Behavior and Effects of Laminar Separation Bubbles on Aerofoils in Incompressible Flow", Journal of the Royal Aeronautical Society, Vol 67, December 1983.

5.50 Wood, Karl Dawson: Aerospace Vehicle Design. Joshua Publishing, Inc., Boulder, Colorado, 1968.

5.51 Yang, T. Y.: Finite Element Structural Analysis. Prentice-Hall, Inc., New Jersey, 1986.

6.0 Program Planning

The necessities of costing the aircraft proposal, program management and future design plans are discussed in Section 6.0

6.1 Budget Considerations

This section summarizes the procedures and methods that were used to analyze the cost aspects of the HAMMER aircraft. Two methods were employed:

1) Statistical methods based on historical data of aircraft
2) Per pound method based on the weight/cost of aircraft

Two statistical methods were employed: One from Reference 5.33 and another from Reference 5.35 the results of these analysis are as follows:

Table 6.1: Cost Estimations (Reference 5.35)

Cost Category	Cost ($1995)
Engineering	162,000,000
Tooling	70,000,000
Manufacturing	45,000,000
Quality Control	6,700,000
Development	42,000,000
Flight Test	4,200,000
Manufacturing Materials	6,000,000
Avionics	500,000
Engine Production	900,000
Total A/C Production Cost	**340,000,000**
Cost per Aircraft	**110,000,000**

Table 6.2: Cost Estimations (Reference 5.33)

Cost Category	Cost ($1995)
Airframe Engineering/Design	57,000,000
Development Support & Test	17,000,000
Flight Test Airplane(s)	256,000,000
Flight Test Operation	1,300,000
Test and Simulation Facilities	0
RDT&E Profit	33,000,000
Finance	33,000,000
Total A/C Production Cost	**398,000,000**
Cost per Aircraft	**99,400,000**

As is evident from the values, the statistical methods yield unrealistic values for the the cost of the XR-1 HAMMER.

Another method to determine the cost was used, using Reference FAA Staticistical Handbook. The market cost for all the civilian aircraft (including jet transports) sold in the United States between 1978-1985 (in 1985 dollars) were summed and divided by the airframe weights of all these aircraft. This yielded a cost per pound of $171.50 that was used to determine the cost of the aircraft based on the empty weight of 11,500 lbs. It was hoped that in using this method the broad range of aircraft would encompass the design of the XR-1 HAMMER (i.e. the large wingspans of commerical jets, the internal combustion engines of general aviation aircraft etc) and yield a reasonable cost per plane. The cost was determined to be $2.26 million per plane.

The unique nature of the aircraft is the reason the cost of the aircraft is difficult to estimate. Statistical methods yield unrealistic results and the per pound method only provides a rought estimate of the costs involved.

6.2 Design Program Plans

The program planning is an essential part of any operation. Without careful planning, there is no direction for the project, and very little is accomplished. Goals must be decided upon at the beginning of the project and modified, if need be, throughout the course of the project as needs present themselves.

For the preliminary design phase of the development of the XR-1 aircraft, the first item of business was to outline the design drivers. Then a plan was formed to work to meet those goals within a certain time frame. A timeline was created that

showed every step of the design process: who was doing the analysis and what the progress was for each of the major areas that was being worked on.

Now that the preliminary design is completed, a new strategy is required to complete the program. The RFP states that the aircraft must be able to go into production by the year 2000. That is, current technology must be used for the design of this aircraft in order to have the aircraft flying and taking data samples as soon as possible. The Gantt Chart in Figure 6.1 shows the program milestones in graphical form.

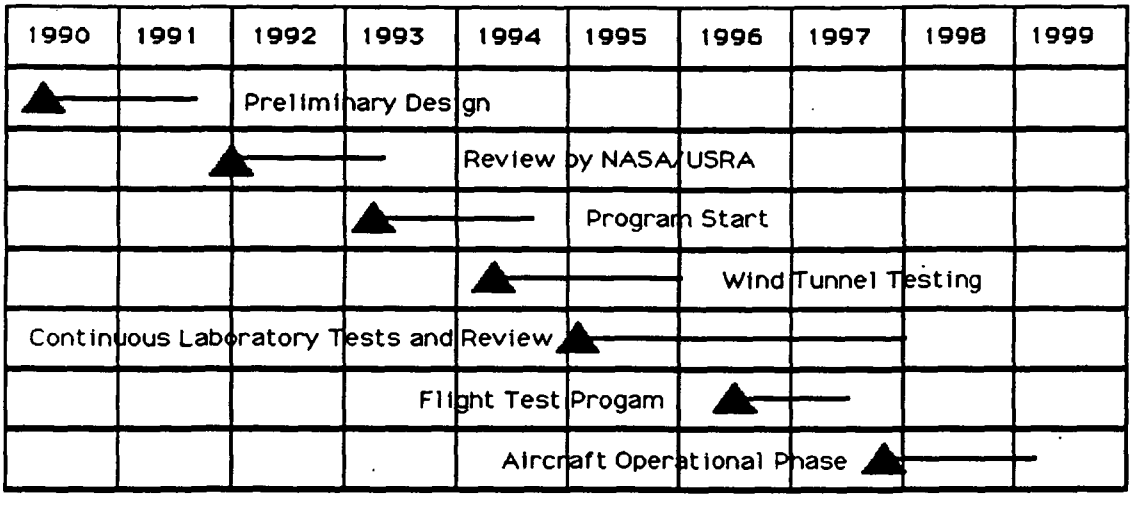

Figure 6.1: XR-1 Program Milestones

To elaborate on the information given in the chart, the preliminary design is completed in 1991 with this report. The preliminary design shows the plan for fulfilling the requirements given in the RFP. It includes all of the preliminary design and analysis for the XR-1 HAMMER.

The next phase of the program is the Program Start which is scheduled to begin in early 1993. In the time between the end of the preliminary design and the

actual program start, NASA will have the chance to review the proposal and determine its feasibility. Once the go-ahead directive is sent out from NASA, the carefully designed plans may be put into effect and the prototype is constructed. The final design plans are to be carried out at NASA Ames Research Center in Moffett Field Naval Air Station, California.

Once a prototype model has been fabricated, (or actually during the process of the manufacturing of the prototype), the wind tunnel testing may begin. This is scheduled to begin in the year 1994 also at NASA Ames Research Center. If these tests do not produce satisfactory results, modifications in the original plans must be made. However, if the wind tunnel testing runs smoothly, the next phase may begin.

The next scheduled phase is the actual flight testing of the aircraft. For the purposes of the missions outlined in the RFP, the testing may be unmanned, so that a systems check may be performed to see how the aircraft behaves if there is a program malfunction or a loss of communication. However, since it would be possible to provide for a pilot for future shorter missions, the restructuring of the cockpit and outfitting for a pilot may commence at the same time as the unmanned flight testing. This is planned to happen in 1996. Both the manned and unmanned testing will be performed at NASA Ames/Dryden Flight Research Center at Edwards Air Force Base in Palmdale, California.

Once the flight testing has been completed to the satisfaction of NASA engineers and the scientists, the operational phase may commence with the first mission being flown in mid-1997. This would be followed by the completion of all four missions as specified by NASA, as well as any additional missions that may be added to the program. All of the missions are expected to be completed well before the year 2000. Should any problems arise in any of the final stages, there will still be enough time to begin the operational flights of the XR-1 HAMMER before the ultimate

deadline set at the end of the decade.

6.3 Manufacturing

Since the XR-1 HAMMER is being built for research purposes only, there is no need for it to go into wide scale production. The probable number of aircraft that would be produced is a minimum of two up to a maximum of about four aircraft. One prototype will be produced along with one or two other aircraft which will be flying the actual missions as described in section three. The prototype would also be capable of performing each of those missions as specified, as it would be a fully-functioning, full-scale model.

Many types of manufacturing methods exist for the production of composite materials. It could be reasonable expected that the majority of these methods will be utilized in the production of the XR-1, since there are so many different types of parts that need to be constructed, depending on the type of composite material that is to be produced and what the required properties of that material must be. Some of these possible methods are described here. The skin of the wings of the aircraft will either use a tape lay-up machine, similar to what is used for the wings of the B-2 bomber, or kevlar or graphite/carbon fiber prepreg laminate. Composites have been around and been in production long enough that these methods have been well tested and well known. The beauty of composites is that no matter how odd the shape of a particular part may seem, composite construction allows for complete freedom without heavy bolts or rivets holding the structure together. The rounded shape of the fuselage is the perfect candidate for a filament-wound structure. This process is somewhat similar to constructing something from paper mache. Some type of mold is made, and the composite fibers are quickly spun and wound around the outside of the shape and the resin (usually epoxy) is applied. The vertical tail

would most likely utilize composite sandwich construction with a kevlar fiber matrix for the skin and a Nomex honeycomb core. This adds stiffness to the structure without adding a lot of weight.

The manufacturing process for the XR-1 will take place at the HAMMER Aerospace Company in Boron, California. The company's close proximity to NASA Ames/Dryden Test Research Facility at Edwards Air Force Base will provide an excellent support base for the aircraft. This will also allow for the research teams involved to be readily available during the manufacturing of the vehicle.

The production of the XR-1 at the HAMMER Aerospace Co. (HAC) is divided into two main Engineering Divisions. The Materials Engineering Division is responsible for the production of the materials responsible for the construction of the aircraft. The Production Engineering Division is responsible for the assembling of sections and eventually the entire aircraft. Both divisions are housed in adjoining buildings to provide independence as well as support for each group. Many of the required tooling devices are different, therefore each division will have its own tooling department.

The Material Engineering Division is capable of handling the development of materials for the vehicle. The manufacturing of prepeg tape , fabric and sandwich elements are the main drivers for this division. The prepeg tape and fabric development will work closely together. This is in result of both portions reliance on the material Spectra 1000. The composite will be developed at the facility and then weaved to create the necessary pieces. This portion is responsible for creation of the shin to the aircraft and to the prepeg tape required for the assemblage of the vehicle. Sandwich elements will work independently from the other because of its reliance on the graphite/epoxy. This section will develop the spars, ribs and stringers that the project uses. Throughout the manufacturing process, the testing facilities will examine all portions of the project that will be used in construction.

The Production Engineering Division is the assembly house for the aircraft. This division is divided into two sections. The first section assembles portions of the aircraft such as the wing, fuselage, and vertical tail. Once these portions are completed, the pieces are sent to the final section, Assembly. Here the aircraft is assembled to its final form. In Assembly, the engines, propellers, landing gear and internal avionics will all be installed on to the airframe.

Once the final assembly is completed, The aircraft will be delivered to NASA Ames/Dryden Flight Test Center for testing, verification, installation of all science equipment. After completion of these tasks, the aircraft is ready to be used on its enivromental research missions.

References:

6.1 Christy, Joe: Aircraft Construction, Repair and Inspection. Tab Books, Blue Ridge Summit, Pennsylvania, 1984.

6.2 Shannon, Robert E.: Engineering Management. John Wiley and Sons, New York, 1980.

7.0 Summary

This section will serve as a brief overview of the design of the XR-1 HAMMER that was presented in the previous sections.

7.1 Analysis Overview

Scientists have been studying the depletion of the Earth's ozone layer for several years with the aid of satellites, balloons, and aircraft. However, in order to better understand the problem, and what corrective measures might be taken, it is necessary to sample the atmosphere in the region of the ozone layer. This cannot be accomplished using any aircraft currently in use since no aircraft exists which can maintain a subsonic cruise at a 100,000 foot altitude for a range of 6000 n mi carrying a payload weighing 2500 pounds. The preliminary designs for an aircraft that is capable of fulfilling the above requirements are contained within the pages of this proposal. This aircraft, called the XR-1 HAMMER, which stands for High Altitude Multiple Mission Experimental Researcher, has been designed to meet the criteria specified in the Request for Proposal (RFP). The comparisons as to what the RFP required and the results that were obtained is seen in Table 7.1.

Table 7.1: RFP Comparsion Chart

RFP ITEM	Requirement	Achievement
MISSION PROFILES	6000 n mi @ 100,000 ft 6000 n mi @ 70,000 ft Zoom to 120,000 ft	Satisfied Satisfied 110,000 ft Maximum
RUNWAY	75 ft maximum width Clear 4 ft obstacles	60 ft Gear Spacing Satisfied
CROSSWINDS	Withstand 15 kt Crosswinds	Satisfied
SPOILERS	Lift Dump Devices	Spoilers Utilized
ENGINES	Minimum of 2	3 IC Engines
HANGAR	110 ft X 70 ft	Detachable Wings
PRODUCTION	By 2000 year	Satisfied

it is readily seen, the XR-1 can meet or exceed all of the requirements as stated in the RFP, with the exception of the zoom up to 120,000 feet. However, the operational ceiling of the aircraft is 110,000 feet, and a safe excursion to even higher altitudes than 100,000 feet is possible. The main restriction on the maximum altitude that can be reached is the engine cooling. At such high altitudes, the cooling system cannot remove the heat from the engine as fast as the engine is producing it. However, due to the fact that the air density is so much less at 100,000 feet than at sea level, in order to climb to higher altitudes would require flying at velocities faster than the speed of sound. Since this is not feasible, especially for a propeller-driven aircraft, it was decided that the highest altitude that could safely be acquired was 110,000 feet, which still allows for some freedom to sample the atmosphere at even higher altitudes and discover how the chemistry of the atmosphere changes with increasing altitude past 100,000 feet.

7.2 Aircraft Design Summary

The XR-1 HAMMER is a tandem-wing, twin boom aircraft designed to cruise at a velocity of Mach 0.65 at an altitude of 100,000 feet for 6000 nautical miles. The purpose of this aircraft is to fly at high altitudes so as to take in-situ data samples of the atmosphere around the region of the ozone layer. Several methods for accomplishing this mission were looked at including the use of satellites, sounding rockets, balloons, and blimps. These were determined to be inadequate for the specified mission profiles. Many types of configurations were also researched, with the tandem wing/twin boom configuration selected as the best choice. In order to keep the weight of the aircraft at an absolute minimum, advanced composite materials will make up the structure of the aircraft. Not only do composite materials weigh less than their metallic counterparts, many have increased strength. A modified Lissaman airfoil was selected in order to obtain a maximum lift coefficient of 1.2. The lift to drag ratio was determined to be 35. Three internal combustion reciprocating engines, a modified version of the Teledyne Continental TSIOL 550 will power the aircraft with the aid of advanced propfan propellers. Through the use of stability augmentation systems, the aircraft will have level 1 flying qualities and have both lateral and longitudinal stability. The aircraft will have retractable landing gear to allow each aircraft to perform multiple missions with a short turn-around time. The aircraft can safely perform the mission profiles as given in the RFP with a maximum zoom altitude of 110,000 feet. The aircraft could enter production almost immediately, with successful flights being flown before the year 2000.

7.3 Concluding Remarks

In conclusion, it must be mentioned that the XR-1 HAMMER is a very feasible solution to the problem of sampling the ozone layer. It is, however, only the first step towards the solution to an even greater problem of the depletion of the ozone layer itself. Great care has been taken in the design of this aircraft, so that no materials or means of propulsion would be used that would further damage the environment any more than was absolutely necessary. This aircraft, on paper, may seem to be just a senior design project and nothing more. Yet, if one looks more closely, it becomes apparent the the future of the entire globe may rest on something as simple as an aircraft that can sample the ozone layer so that scientists may interpret this data into a plan for survival and perhaps the reconstruction of the ozone layer.

The design of this aircraft has been an enlightening experience for all of those invovled with the project. However, this project may never have been completed without the help of certain people. Special thanks goes to NASA/USRA for supplying the original idea for this study, to Professor Paul A. Lord whose guidance and support saw the project through to the end, to Teledyne Continental for their generosity in sharing information concerning the engine, and, finally, to all of the team members who worked so hard to see it all come together.

Appendix